FYS-KJM4740

MR Spectroscopy and Tomography – Part I

Eddy W. Hansen (and Bjørn Pedersen)

The new (2010) solid-state NMR spectrometer located at SINTEF Oslo, which is available for researchers at KI/UiO/Sintef.

Department of Chemistry
University of Oslo
January 2014

Table 1.2 Acronyms and abbreviations

BEST	Blipped echo-planar single-pulse technique
BOLD	Blood oxygen level dependent contrast
BURP	Band-selective, uniform response, pure-phase pulse
COSY	Correlation spectroscopy
CP-MAS	Cross-polarization with magic angle spinning
CPMG	Carr–Purcell–Meiboom–Gill
CSF	Cerebrospinal fluid
DOSY	Diffusion-ordered spectroscopy
EXSY	Exchange spectroscopy
fMRI	Functional magnetic resonance imaging of the brain
HMQC	Heteronuclear multiple-quantum correlation
HOHAHA	Homonuclear Hartmann–Hahn technique
HPLC	High-performance liquid chromatography
HSQC	Heteronuclear single-quantum correlation
INADEQUATE	Incredible natural abundance double-quantum transfer experiment
INEPT	Insensitive nuclei enhanced by polarization transfer
ISIS	Image-selected *in vivo* spectroscopy
MLEV	Malcolm Levitt's phase cycle
MRI	Magnetic resonance imaging
MRS	Magnetic resonance spectroscopy
NOESY	Nuclear Overhauser enhancement spectroscopy
NMR	Nuclear magnetic resonance
PRESS	Point-resolved spectroscopy
ROESY	Rotating-frame Overhauser enhancement spectroscopy
STEAM	Stimulated echo acquisition mode
TOCSY	Total correlation spectroscopy
WAHUHA	Magic pulse cycle of Waugh, Huber and Haeberlen
WALTZ	Wideband alternating-phase technique for zero splitting
WURST	Adiabatic soft radiofrequency pulse shaped like a sausage

Some of the many acronyms and abbreviations used in MR (Freeman, 2003)

Preface

NMR is an exciting and challenging experimental technique which is also intellectually demanding. The present booklet is intended for students taking the course FYS-KJM 4740 *MR-theory and medical diagnostics* in spring 2009 and covers the first 12 hours of lectures. It gives a comprehensive introduction to the basic theory and concept of Magnetic Resonance (MR).

The first lecture note was prepared in 1977 (in Norwegian) while the present document represents a fourth and significantly modified version of the first English edition. The content has been adjusted according to the MR equipment available at the Department of Chemistry and to the ongoing research activities at the Laboratory for Physical MR. In particular, application of MR spectroscopy (MRS) to probe diffusion is discussed more thoroughly in this last version of the lecture note.

Since the application of gradient pulses has become a “must” in both MR-spectroscopy (MRS) and MR-imaging (MRI), we find the theory of diffusion to represent a soft conceptual transition from the field of MRS to MRI.

We will appreciate any response from the student concerning typographical errors or obscurities in the text. So please, send your remarks to: eddywh@kjemi.uio.no .

Oslo, January 2014

Eddy W. Hansn

Content

1. MR – Application and instrumental design

1.1 Applications of magnetic resonance (MR)

Since 1938 Nuclear Magnetic Resonance (NMR or MR[1]) has found an increasing number of applications, as illustrated on Figure 1.1. Chemical applications are found on the left and medical applications on the right. The two areas are not distinct, but are largely overlapping. However, the applications are becoming increasingly more specialized and are frequently divided into separate subjects and professions. In this course, however, we will concentrate on the more fundamental aspects of NMR and present some examples from the research activities of the authors NMR spectroscopy of substances in solution, often called high-resolution NMR, is the most frequently applied technique to probe the *type* of molecules, the *number* of molecules and the *structure* of molecules in solution. Also, the *motional characteristics* (translational, rotational) of the molecules and any dynamic equilibrium can be probed by NMR. Because the molecular motion averages out certain interactions, as will be explained later, the peaks observed in the spectra are very narrow. (The peaks are also called lines as in optical spectroscopy.). Thus, the technique is called *high resolution* NMR In contrast, the NMR peaks observed from solids are usually broad and featureless leading to the term: wide line NMR or solid-state NMR. By introducing some rather ingenious experimental modifications it is, however, possible to narrow the peaks from solids so the underlying fine structure can be made observable. NMR spectra of solids may also give information on the structure and motion (hindered rotation and diffusion) of the molecules, ions or atoms confined in the solid state.

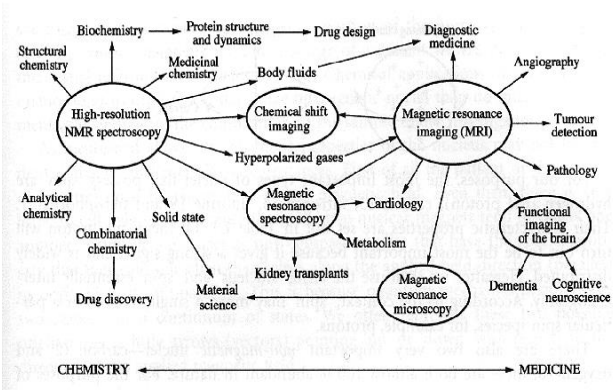

Figure 1.1 *Applications of MR/MRI*

Additionally, MR is also capable of producing images of three-dimensional objects with a resolution of 0.1 mm of large objects, like the human body (MRI) and down to 10 µm of smaller objects of dimension 1 cm (MR-microscopy). To extract this information one needs a radio transmitter and a radio receiver and the sample must be located in a magnetic field as illustrated on Figure 1.2. The magnet is the largest and most expensive part of the equipment making MR expensive comparedto other analytical equipment. Thanks to the development of micro-electronics that has given better and more sensitive radio-transmitters and receivers, combined with the development of new materials that has given stronger and more stable magnets , and the development of cheaper computers that can collect and handle larger amounts of data, MR has improved immensely since the first NMR-signal was detected in 1938. During the last 35 years the sensitivity has increased by more than a million! At the end of this booklet we have briefly summarized the history of MR from the beginning of 1920-to the present day. Many scientists have contributed, and numerous surprising and

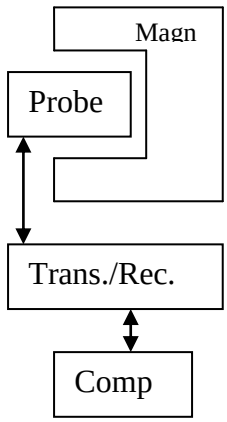

Figure 1.2*. Set up*

[1] Nuclear Magnetic Resonance. In medicine nuclear is usually associated with radioactivity. Therefore the N is dropped. (The use of radioactive compounds for medical purposes is called nuclear medicine.)

unexpected breakthroughs have appeared during the years. Most importantly, however, this development has not yet reached the end. Very likely, there are still new methods to be developed and new applications to be found that may surprise both the scientific community, as well as people in general!
Imaging (MRI) is mostly used in medicine as a forceful diagnostic tool, without the health risk connected to the use of ionizing radiation (X-rays) used in a CT (computer tomography). Moreover, MRI (also called a magnet tomograph) does not only acquire images. If necessary equipment is available, also ^{1}H- and/or ^{31}P-spectra of the object, or part of the object, can be recorded. The goal is to combine the two methods in order to first acquire a 3D-image which reveals the morphology of the object. Then to zoom in on the most interesting parts (f. ex. a small tumour) of this object in order to acquire a spectrum which may give further information on the chemistry taking place in this part.

Due to the broad range of applications of MR, a large number of textbooks are available. In the university library (BIBSYS) 347 references containing the phrase *magnetic resonance* were found. 63 of these were published in 2000 and after (pr 10.01.2005). Some references are summarized at the end of this booklet. You can also find review articles in different journals and yearbooks. Your choice of book(s) to acquire will depend on your background and the goal(s) of your study. The lecturer may give you further information.

1.2 A modern (MR) spectrometer

Figure 1.3 shows the relevant parts of a modern solution-NMR-spectrometer with a super-conductive magnet (right) to a computer (left). The sample is introduced from the top of the magnet and may be located within the magnet by an automatic sample changer. The basic rf-frequency is locked to the magnetic field by a ^{2}H-lock and makes the system more stable to any drift in the magnetic field, or the rf-frequency. ADC is the analogue to digital converter. Usually the spectrometer is equipped with several probes tailored for different purposes. To study solids one needs to generate rf-pulses of large amplitude to reduce the 90^{o}-pulse down to 1 μs. This is because T_2 may be of the order of microseconds and not seconds as for liquids.
Hence, solid state NMR spectrometer necessitates more powerful radio-transmitters.

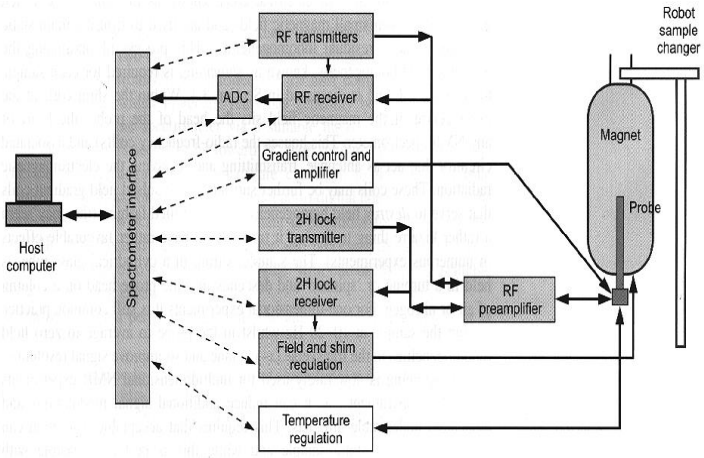

Figure 1.3. *Relevant parts of a solution-NMR-spectrometer*

1.3 MR - basic concepts

1.3.1 The Spin

MR is based on the fact that all materials are built up of electrons and atomic nuclei possessing *angular momentum* and *magnetic dipole moment (Figure 1.4)*. The angular momentum **L**

Figure 1. 4*. A nuclear magnetic dipolemoment* $\boldsymbol{\mu}$*, as formed by a combination of the internal spin and the the charge of the nucleus which resukts in a current i.*

is a characteristic property of the nucleus just like its mass and charge. Moreover, an atomic nucleus with angular momentum also possesses a magnetic dipole moment $\boldsymbol{\mu}$[2] The magnetic dipole moment $\boldsymbol{\mu}$ (a vector) is parallel to its angular momentum **L** (see Exercise 1):

$$\boldsymbol{\mu} = \gamma \mathbf{L} \qquad (1.1)$$

γ is the ratio between the magnetic moment of the nucleus and its angular momentum. γ is termed the *gyromagnetic ratio*. It has been determined experimentally for all isotopes and can be found in tables. In the literature it is common practice to call a particle possessing an angular momentum and a magnetic dipole moment, *a spin*.An example of a macroscopic object having a magnetic dipole moment is a small rod magnet and/or a loop of wire (with current). A loop of wire enclosing an area of b m^2 and carrying a current of 1 A (ampere) will have a dipole moment equal to 1 bA m^2. Therefore the SI-unit for magnetic dipole moment is A m^2.

1.3.2 The MR phenomenon – classical mechanics

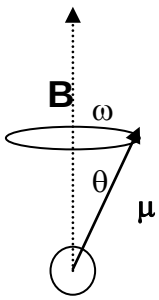

Figure 1.5

In a magnetic field **B** a spin will attain a potential energy which depends on the orientation of the magnetic dipole moment $\boldsymbol{\mu}$ relative to **B**.[3] The potential energy is[4]:

$$E = - \boldsymbol{\mu} \cdot \mathbf{B} = - \mu B \cos\theta \qquad (1.2)$$

θ is the angle between $\boldsymbol{\mu}$ and **B** as shown in Figure 1.5. The equation that describes the motion of the dipole $\boldsymbol{\mu}$ in a magnetic field **B** (see Exercise 2) reads:

$$d\boldsymbol{\mu}/dt = \gamma \boldsymbol{\mu} \times \mathbf{B} \qquad (1.3)$$

This is a differential equation that can be solved when given the initial conditions. If $\mathbf{B} = \mathbf{B}_o$ (constant, i.e. independent of time), and $\boldsymbol{\mu}$ makes an angle θ with the magnetic field, the

---

[2]We use a bold letter for a vector as $\boldsymbol{\mu}$ in this booklet.

[3]The correct name for B is the magnetic flux density and the unit for B is tesla (T). Also the older unit gauss (G) some times is used: 1 T = 10^4 G. Using the basic SI-units 1 T = 1 kg/(As^2). The unit for μ is Am^2. The product μB is then joule (J = kg $(m/s)^2$). (Remember that μB is the potential energy of μ in B.)

[4] $\boldsymbol{\mu}$ x **B** is called the vector product between $\boldsymbol{\mu}$ and **B** and is directed along a unit vector orthogonal to the plane determined by the two vectors $\boldsymbol{\mu}$ and **B**, respectively. It norm or length is defined by $|\boldsymbol{\mu} \times \mathbf{B}| = \mu B \cdot \sin\theta$. The scalar- or dot product between $\boldsymbol{\mu}$ and **B** is definen by $\boldsymbol{\mu} \cdot \mathbf{B}$.

solution is that μ rotates (precesses) about $\mathbf{B_0}$ with an angular velocity ω_0 (see Exercize 1.2) given by:

$$\omega_0 = -\gamma \mathbf{B}_o \qquad (1.4)$$

and represents a particularly important equation in MR. The equation shows that the angular velocity ω_0 is proportional to the magnetic field strength B_0 with a proportionality constant γ, the gyromagnetic ratio. This angular frequency is called the Larmor frequency.[5]

Table 1.1. *MR-data for some isotopes*			
Isotope	**I**	**Abundance** in %	**γ** in 100·radMHz/T
^{1}H	1/2	99.985	2.67510
^{2}H	1	0.015	0.41064
^{13}C	1/2	1.108	0.67263
^{14}N	1	99.63	0.19324
^{15}N	1/2	0.37	-0.27107
^{19}F	1/2	100.0	2.51665
^{23}Na	3/2	100.0	0.70760
^{31}P	1/2	100.0	1.08290
^{39}K	3/2	93.10	0.12484

MR-data for some of the most popular nuclei are given in Table 1. Using Eq 1.3 we notice that $d\mu/dt \cdot \mathbf{B}_0 = d(\mu \cdot \mathbf{B}_0)/dt = (\mu \times \mathbf{B_0}) \cdot \mathbf{B}_o = 0$. i.e., θ in Eq 1.2 is constant.

Classical physics tells us that the spin in a magnetic field will behave in the same way as a spinning top in the gravitational field (Figure 1.6).

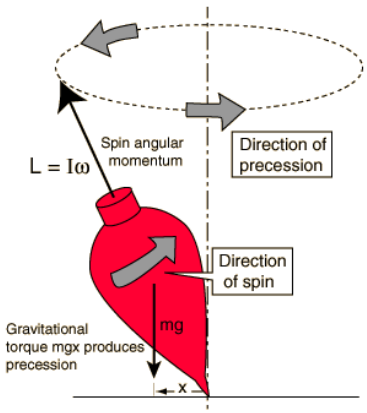

Figure 1.6*. Spinning in a gravitational field*

1.3.3 The NMR phenomemon – quantum mechanics

Nature has shown us that a nuclear spin, defined by a spin quantum number I, can only take 2I+1 different directions in space.[6] The quantum number I is known for all stable

[5] Named after Sir Joseph Larmor (1857-1942) who first performed the classical calculation in 1895.
[6] What nature has taught us is summed up in the quantum theory.

isotopes. In particular, isotopes with a spin quantum numer I equal to 0 have no magnetic dipole moment and do not precess, and is therefore invisible to MR. ^{12}C and ^{16}O are two such nuclei.[7] An isotope with I = 1/2 can take two directions. ^{1}H, ^{13}C, ^{15}N, ^{19}F and ^{31}P are examples of such spin-1/2 nuclei[8] and are the simplest and also the most studied nuclei in MR.

From a quantum mechanical point of view we may define an energy operator or Hamiltonian operator $\hat{H}$ according to the Schrödinger equation:

$$\hat{H}|\Psi> = E|\Psi> \qquad (1.5)$$

where E is the energy and $|\Psi>$ is the spin wave function. For a single spin interacting with a magnetic field B_0 (directed along the z-axis) the Hamiltonian is denoted $\hat{H}_Z$, where Z stands for Zeeman[9]. From classical mechanics the energy E takes the form $E= - \boldsymbol{\mu} \cdot \mathbf{B_o}$ and $\boldsymbol{\mu} = \gamma \mathbf{L}$. By replacing **L** by its quantum mechanical analogous $\hbar \bar{I}$, where $\hbar$ is Planck's constant and I is the spin operator[10], we may write Eq 1.5 in the form:

$$\hat{H}_Z = - \boldsymbol{\mu} \cdot \mathbf{B_o} = -\gamma \mathbf{L} \cdot \mathbf{B}_0 = -\gamma B_o \hbar \bar{I}_z \qquad (1.6)$$

For I = ½ particles there are two eigenstates, defined by the spin wave functions $|\alpha>$ and $|\beta>$, respectively:

$$\bar{I}_z|\alpha> = \tfrac{1}{2}|\alpha> \qquad (1.7a)$$

$$\bar{I}_z|\beta> = -\tfrac{1}{2}|\beta> \qquad (1.7b)$$

Hence, we may calculaties the corresponding two energies, according to:

$$\hat{H}_Z|\alpha> = -\gamma B_o \hbar \bar{I}_z|\alpha> = -\gamma B_o \hbar/2|\alpha> = E_+|\alpha> \qquad (1.7c)$$
$$\hat{H}_Z|\beta> = -\gamma B_o \hbar \bar{I}_z|\beta> = \gamma B_o \hbar/2|\beta> = E_-|\beta> \qquad (1.7d)$$

Hence,
$E_+ = -\tfrac{1}{2} \gamma B_0 \hbar$ and $E_- = \tfrac{1}{2} \gamma B_0 \hbar$

where E_+ is the energy for the state where the magnetic dipole moment is parallel to the magnetic field and E_- is the energy for the magnetic dipole oriented anti-parallel to the external field, as illustrated in Figure 1.7. To produce the actual resonance

---

[7] An isotope where the number of protons and neutrons is an equal number has I = 0. The explanation is that both protons and neutrons have angular momentum, but because they are paired antiparalell in the nucleus the result is 0.

[8] An electron is also a spin 1/2 particle. So atoms with an unpaired electron can be studied with MR. Because the magnetic moment of an electron is about 2000 times larger than the proton magnetic moment the equipment used to study unpaired electrons are different from the equipment used for NMR (radio frequencies in NMR and microwave frequencies in ESR). Electron-MR is called ESR (Electron Spin Resonance) or EPR (Electron Paramagnetic Resonance). At UiO there are two EPR-spectrometers in the biophysics group in the Department of Physics (se http://www.fys.uio.no/biofysikk/eee/esr.htm). They are located two stories above the Physical NMR Laboratory.

[9] The Dutch physicist Pieter Zeeman (1865-1943) discovered in 1896 that certain spectral lines split when the sample was placed in a magnetic field. That is called the Zeeman Effect.

[10] $h = 662.6176(36) \cdot 10^{-36}$ Js. $\hbar = h/(2\pi)$

phenomenon, an alternating magnetic field B_1 is applied perpendicular to the static field B_o, which introduces a perturbing term in the Hamiltonian:

$$\hat{H}_{pert} = - \gamma B_1 \hbar \bar{I}_z \qquad (1.7e)$$

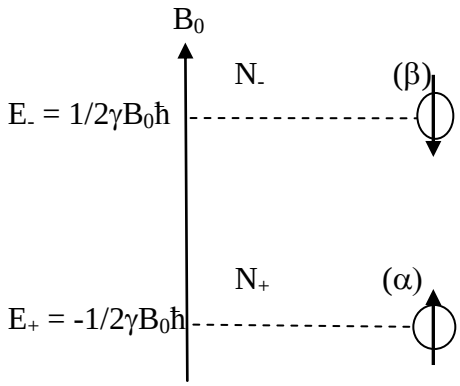

Figure 1.7*. Energy levels (E_+, E_-) and and spin-populations (N_+, N_-) of spin-states α and β.*

Hence, using electromagnetic radiation with the correct frequency the spins will change orientation in space. The energy in electromagnetic radiation comes in packets called photons having energy $h\nu$, where ν is the radiation frequency and h is Planck's constant. Hence, the energy difference between the two eigenstates reads:

$$\Delta E = (E_- - E_+) = \hbar\omega = h\nu = \gamma B_0 \hbar \text{ or } \omega = \omega_0 = \gamma B_0 \text{ (note: } \omega = 2\pi\nu) \qquad (1.7f)$$

and defines the basic equation in MR, the Larmor equation. The radio stations, i.e., the Larmor frequencies in a "MR-radio" are wider spaced than in an ordinary radio,[11] and can only be tuned to one type of nuclei at a time, for instance either protons or carbons. We notice that the basic equation describing the resonance phenomenon is the same whether derived from classical physics or quantum physics. One model is not better than the other. Actually, both models are used in tandem to explain different MR observations, making the MR-language somewhat special.

The basic equation shows that when a nuclear spin in a magnetic field is exposed to electromagnetic radiation with the right frequency (Larmor frequency), an exchange of energy between the spins and the radiation takes place. This exchange of energy is called resonance and the frequency is denoted the resonance frequency.[12]
In a 1.5 T field the resonance frequency for the protons is 64 MHz[13]. All other isotopes have a resonance frequency that is smaller, as shown in Table 1.2. However, all frequencies are in the radio frequency range (MHz).

[11]The FM-band stretches from 88 to 108 MHz

[12]We are mostly acquainted with resonance in a mechanical system. When a glass scatters of a note it is because the note corresponds to one of the resonance frequencies of the glass.

[13]1 MHz = 10^6 Hz. 1 Hz = 1 s^{-1}. Hz = hertz.

Table 1.2. *Resonance frequency of ^{1}H and some other isotopes in a 1.5 T magnetic field[14].*

	Table 1.2. *The resonance frequency at 1.5 T*
Isotope	**Resonance frequency**/MHz
^{1}H	63.9
^{2}H	9.8
^{13}C	16.1
^{14}N	4.6
^{15}N	6.5
^{19}F	60.1
^{23}Na	16.9
^{31}P	25.9
^{39}K	3.0

1.3.4 The spin system

A sample will contain many spins (Avogadros number). Since each spin, or magnetic dipole, generate its own magnetic field, each spin in the system will experience the external magnetic field as well as the magnetic field set up by all its neighbouring spins. This local field will in general be smaller than the external field.[15] However, we can continue to describe the collection of spins in the sample on the basis of the energy levels given for a single, isolated spin. If denoting the collection of spins of the same type in the sample a "spin-system" it may be uniquely described if knowing the number of spins (N_+) in the lowest energy level since the number (N_-) of spins in the highest energy level will then be equal $N_0 - N_+$ where N_0 is the total number of spins in the system.
Such a spin system can be described in a thermodynamic sense by the Bolzmann equation:

$$\frac{N_-}{N_+} = \exp\left[-\frac{\Delta E}{kT}\right] = \exp\left[-\frac{\hbar\gamma B_0}{kT}\right] \qquad (1.8a)$$

Since $\mu B << kT$, we may write:

$$N_+ = \frac{N_0}{2}\left[1 + \frac{\hbar\gamma B_0}{2kT}\right] \qquad (1.8b)$$

$$N_- = \frac{N_0}{2}\left[1 - \frac{\hbar\gamma B_0}{2kT}\right] \qquad (1.8c)$$

Moreover, because $N_+ + N_- = N_0$ then:

$$\Delta N = N_+ - N_- = \frac{\gamma\hbar B_0 N_0}{2kT} \qquad (1.8d)$$

where ΔN is the difference in population between the two energy levels, i.e., the surplus of spins in the lowest energy level.

---

[14] 1 MHz = 10^6 Hz. 1 Hz = 1 s^{-1}. Hz = hertz.

[15] This is one example of a local magnetic field. In the next chapter we will present other local fields.

We will later show that we can change the population in each level by irradiating the spins. By turning all spins 180^o the population difference will change sign. Thermodynamically the system can still be described by the Boltzmann distribution if accepting a negative absolute temperature (It requires energy to turn all spins). Consequently, a negative temperature is hotter than a positive temperature when the system is in thermal equilibrium![16]

We define a macroscopic magnetic dipole moment **M** as a (vector)-sum of all the dipole moments (or spins) in the spin system. At equilibrium **M** will be parallel to $\mathbf{B_0}$ and reads: $\mathbf{M} = (\Delta N \boldsymbol{\mu} \cdot \mathbf{k})\mathbf{k}$ where **k** is a unit vector along $\mathbf{B_0}$ (defined as the z-axis). **M** is an important quantity in MR and forms the basis for the observable MR-signal.

Einstein showed that when a photon passes through a spin system the probability for absorption of the photon will be equal to the probability that a similar photon is emitted. Hence, a signal is detectable only when a population difference exists (absorption when $\Delta N > 0$ and emission when $\Delta N < 0$).

1.3.5 The Free Induction Decay (FID)

The motion of the macroscopic magnetization **M** is governed by the same physical laws as for an individual magnetic dipole (Eq 1.3). Hence,

$$d\mathbf{M}/dt = \gamma \mathbf{M} \times \mathbf{B_0} \qquad (1.9)$$

However, it can be shown (lecture) that the macroscopic magnetization component $M_\perp$, normal to the static magnetic field $\mathbf{B}_0$, is zero. Since the receiver coils is placed normal to $\mathbf{B}_0$, there is no sample magnetization to be detected. So, how can we actually probe the NMR signal?
The answer is that the macroscopic magnetization aligned along $\mathbf{B}_0$ (z-axis) must – somehow - be tilted, or flipped, or rotated into the xy-plane where the receiver coil is located. One way of performing this "tilt" is to apply a magnetic field B_1 in the xy-plane, for instance, along the x-axis. Importantly, this magnetic field must oscillate with a frequency ω (around the z-axis) which is close to the Larmor frequency ω_0**.** This can be accomplished by sending an alternating current of frequency ω and amplitude B_1 into the coil, as illustrated on Figure 1.8. The oscillating magnetic field generated in this way may be regarded as composed of two rotating magnetic fields with opposite directions, as illustrated in Figure 1.8 (right). Only the B_1-field component rotating in the same direction as **M** will influence **M** and suggests that the macroscopic magnetization **M** will experience two magnetic fields, one static magnetic field ($\mathbf{B}_0$) and one rotating magnetic field $\mathbf{B}_1$.

[16] If you choose –1/T as a horizontal temperature scale you will get a better scale to understand this. The low temperatures will be to the left and the high temperatures to the right. Then it is also easier to understand that you will never get to 0 K as this will be at minus infinity.

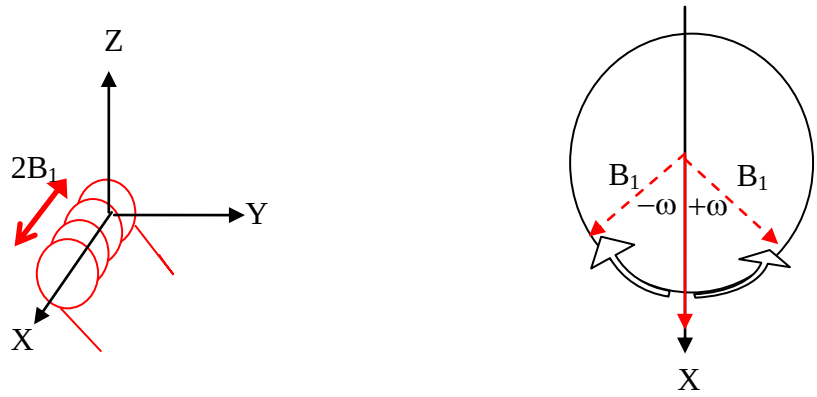

***Figure 1.8**. left: Coil arrangement with a linearly polarized (alternating) current along the x-axis. right: Decomposition of the alternating current into two oscillating magnetic fields with frequency ω and $-\omega$ (rotating in opposite directions).*

To vizualise the motion of the magnetization **M** in a system of two orthogonal magnetic fields $\mathbf{B}_0$ and $\mathbf{B}_1$ is not too complex. It is simply composed of two independent rotations of circular frequencies $\boldsymbol{\omega}_0$ (= $-\gamma B_0\mathbf{k}$) and $\boldsymbol{\omega}_1$ (= $-\gamma B_1\mathbf{i}$) around the z-axis and the x-axis, respectively. However, this motion can be significantly simplified if viewing the motion in a coordinate system (uvz) rotating around the z-axis with frequency $\boldsymbol{\omega}$ (= $-\omega\mathbf{k}$), i.e., the same frequency as the oscillating B_1 field. In this rotating frame of reference $\mathbf{B}_1$ is directed along the u-axis and $\mathbf{B}_o$ is directed along the z axis. It can be shown that in this rotating frame of reference the magnetization can be considered to experience or sense an apparent or effective magnetic field $\mathbf{B}_{eff}$ which can be written:

$$\mathbf{B}_{eff} = B_1\mathbf{u} + (B_O - \omega/\gamma)\mathbf{k} \qquad (1.10)$$

where $\omega_0 = \gamma B_0$ (Figure 1.9; left). We notice that in the rotating coordinate system all magnetic fields can be considered constant and independent of time. Of particular interest is the situation when on resonance ($\boldsymbol{\omega} = \boldsymbol{\omega}_0 = -\gamma\mathbf{B}_0$) because then only the B_1 field along the u-axis is non-zero. As long as B_1 is turned on, this causes a presession (rotation) of the magnetization around the negative u- axis with a resonance frequency $\boldsymbol{\omega}_1 (= -\gamma B_1 \vec{u})$ as illustrated on Figure 1.9 (right). It follows that the angle (α) of rotation (phase angle) of **M** around the negative u-axis after time t is:

$$\alpha = \omega_1 t = \gamma B_1 t \qquad (1.11)$$

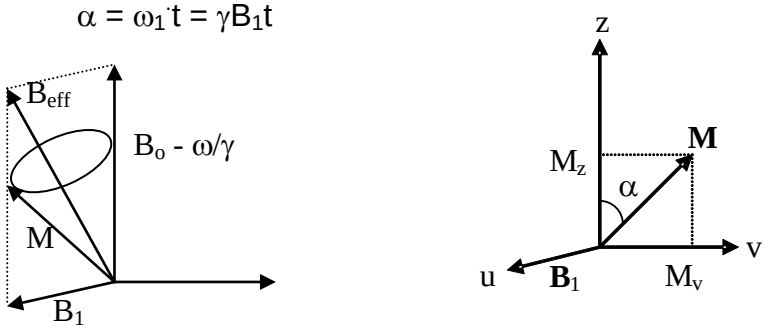

Figure 1.9. Rotation of a macroscopic magnetic moment **M** around the effective magnetic field B_{eff} (left) and the corresponding rotation of **M** around $\mathbf{B}_1$ when on resonance ($B_o - \omega/\gamma = 0$; right).

If the radio pulse is on for a time t_{90}, which corresponds to the magnetization being rotated an angle $\alpha = \pi/2$ (a so called "90^0 rf-pulse), the magnetization **M** will be directed along the v-axis in the rotating frame. This signal can then be detected by a receiver coil placed along the x- or y- axis in the laboratory frame.

As $M_z = \Delta N \cdot \mu_z$, the signal intensity will be proportional to $\frac{\gamma^2 \hbar^2 B_0 N_0}{4kT}$ (Exercise 1.3). As a consequence, the signal intensity increases with the strength of the external magnetic field B_0 and it will become stronger for those nuclei that have the larger γ. This latter implies that ^{1}H and ^{19}F will give a stronger signal than ^{13}C and ^{15}N (see Table 1.1). Furthermore the signal is proportional to N_0, the number of spins confined in the receiver coil. N_0 will be proportional to the density of spins, which in turn depends on the isotopic abundance of these spins (see Table 1.1). The abundance can be increased by isotope enrichment. We will return to this point in a later chapter when discussing the signal-to-noise ratio.

Also, a 90^o- pulse that last a few microseconds (μs) is called a hard or non-selective pulse, while a 90^o- pulse that last a few milliseconds (ms) is called a selective or soft pulse.[17] A hard pulse covers a larger frequency range and will be commented on in a later section.

1.3.6 MR detection

How then can we detect the x- and y-components of the oscillating (magnetization) signal: $I_S = I_0 \cdot \exp[-i\omega t]$ (= $I_0 \cdot \cos \omega t\vec{i} + I_0 \sin \omega t\vec{j}$) when only one receiver coil (along the x-axis) is applied? That is, only the signal $I_S^R = I_0 \cos \omega t$ along the x-axis is sampled. One option is to have two coils, one along the x-axis and the other along the y-axis. However, such an arrangement is practically difficult to realize. There exists, however, an internally generated oscillating signal I_{REF} of frequency ω_0, i.e., $I_{REF} = \exp[-i\omega_0 t]$ (= $\cos \omega_0 t\vec{i} + \sin \omega_0 t\vec{j}$) By mixing (multiplying) the two signal (see Figure 1.10) and filtering out the high frequency component ($\omega+\omega_0$), we obtain the twe rotating frame signals $S_U = I_0 \cdot \cos((\omega - \omega_0)t)$ and $S_V = -I_0 \cdot \sin((\omega - \omega_0)t)$ which are stored in two separate channels, denoted U and V, respectively (see Problem 1.6). As can be noted, the two signals S_U and S_V are phase shifted by 90^0.

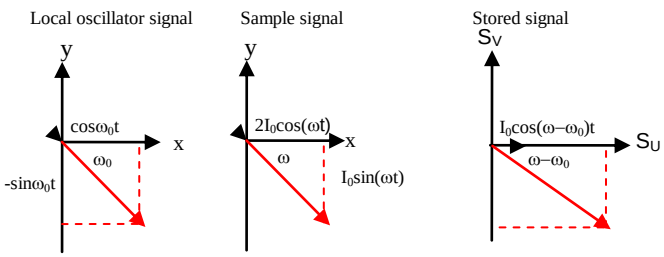

***Figure 1.10**. Illustration of the local oscillator signal, the sample signal and the resulting two signals U and V stored in the computer.*

[17] 1 μs = 10^{-6} s

1.4 Exercises

1.1) Try to argue why **μ** = γ**L** by applying the well known result that the magnetic dipole moment (μ) formed by a closed current loop (i) is proportional to the current times the area(A) defined by the current loop, i.e., μ = iA (assume a circular current loop).

1.2) Discuss the motion of a magnetic dipole **μ** in a magnetic field $\mathbf{B_0}$, i.e., derive the equation; d**μ**/dt = γ**μ** x $\mathbf{B_0}$ by combining the angular momentum **L (= r x** m**v)** and the torque τ = (**r** x **F = μ** x $\mathbf{B_0}$**)**.

1.3) Show that the macroscopic magnetization M can be approximated by the formula:

$$M \propto \frac{1}{4kT}(\gamma h)^2 B_0 N_0$$

1.4) Describe the motion of the magnetic dipole moment μ in the rotating frame of reference by solving the Equation:

$$\frac{d\boldsymbol{\mu}}{dt} = \gamma \boldsymbol{\mu} x \mathbf{B}_{eff} \qquad when \qquad \mathbf{B}_{eff} = (B_0 - \omega / \gamma)\mathbf{k}$$

where -ω**k** defines the frequency of the rotating frame of reference.

1.5) What is the effect of a linearly polarized magnetic field $\mathbf{B_1}$= B_1cosωt **i** (in the laboratory frame (xyz)) on the magnetic dipole moment μ, when "on resonance", i.e., $\omega = \omega_0$. (Hint. Use the rotating frame concept)

1.6) An internally generated oscillating signal $I_{RX}\ (= \exp(-i\omega_0 t))$ of frequency ω_0 is multiplied by the detected sample signal $I_S = 2I_0 \cos(\omega t) = I_0 \exp(i\omega t) + I_0 \exp(-i\omega t)$. Show that the resulting mixed signal S takes the form:

$S = I_0 \cos[(\omega_0 - \omega)t]\vec{i} - I_0 \sin[(\omega_0 - \omega)t]$.

(Hint: The high-frequency component $|\omega_0 + \omega|$ is filtered out by using a low-pass filter. See also notes from the lecture!)

2. Bloch equation and relaxation

2.1 Spin-spin relaxation time - T_2

From the discussion above, we found that after a 90°-pulse **M** will precess around $\mathbf{B}_o$, and will induce a current in the coil. This current will be an alternating current which varies with the resonance frequency. It also follows that the amplitude of the current will stay constant. This is, however, unreasonable since “nothing can last for ever”. What will then make the signal decay? We know that **M** will be directed along $\mathbf{B_o}$ when the system is at equilibrium. Since the 90°-pulse has brought the system out of equilibrium, how will the spins find their way back to equilibrium? We will now try to give the answers to these two questions.

M represents the vector sum of all spins in the sample. The magnetic field experienced by each spin is the sum of the external field (B_o) and a local field from the neighbouring spins (B_{lok}). The external field is the same for each spin, but the local field may vary from one spin to another because it depends on the relative orientation of the neighbouring spins. (We will describe the local field in more detail in the next chapter). Because the resonance frequency is proportional to the magnetic field experienced by the actual spin ($B_o + B_{lok}$), the spins sensing a large local field will necessarily precess faster than spins experiencing a smaller local field. This means that the components of **M** in the rotating coordinate system will spread out in the xy-plane with time, due to loss of phase coherence, causing the resultant M to decay. A simple assumption is that M will decay exponentially with time (Figure 2.1)

$$M = M_o e^{-t/T_2} \qquad (2.1)$$

T_2 is called the spin-spin relaxations time and is an important time parameter in NMR.

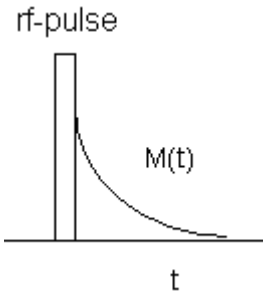

Figure 2.1 *Signal decay after application of an rf-pulse*

We note that when $t = T_2$ the signal intensity will be reduced by a factor e^{-1} (e = 2.7183) relative to its initial value.

2.2 Spin-lattice relaxation - T_1

The other question we asked was how long time it takes for a spin-system to relax to equilibrium after being perturbed. The answer is related to moelcular motion through the time variation of the local magnetic field B_{lok}. For instance, the local magnetic field set up by the combined effect of electron currents within the molecule and the molecular motion will fluctuate with time. Of particular importance, the fluctuation frequency of these local magnetic fields which accurately matches the larmor frequency of the spins will be the most effective source of relaxation. For simplicity,

we will assume the macroscopic magnetization to return to equilibrium exponentially with respect to time, after being perturbed by for instance an rf-pulse (Exercise 2.7) Actually, it can be shown that after the magnetization is first perturbed by an rf-pulse which tip the magnetization an angle θ relative to the external field, the magnetization M_Z along the static magnetic field will increase with time according to:

$$M_z = M_o(1-(1 - \cos\theta)\, e^{-t/T_1}) \qquad (2.2)$$

where T_1 is called the spin-lattice relaxation time and is an important MR-parameter.

Within the rotating frame of reference, we may summarize: Before a 90°-pulse $M_z = M_o$ and $M_x = M_y = 0$. Immediately after applying a 90°-pulse $M_z = 0$, $M_x = 0$, and $M_y = M_o$. After a time $t >> T_1$ it follows that $M_x = M_y = 0$ and $M_z = M_o$ and the system has returned back to equilibrium.

The signal detected in the radio receiver will be at a maximum immediately after the rf-pulse and later decay as shown in figure 2.2. Because the signal is detected after the transmitter has been turned off the signal is called a *free induction decay* (fid). Interestingly, we can determine T_2 by analyzing the decay of this fid.

One frequently approach to measure T_1 is to expose the spin system to a 90°-rf-puls, a time τ after applying a 180^0 pulse, and then monitor the time behaviour of M_z as a function of τ (Figure 2.3). This is denoted an Inversion Recovery pulse sequence and is illustrated in Figure 2.2).

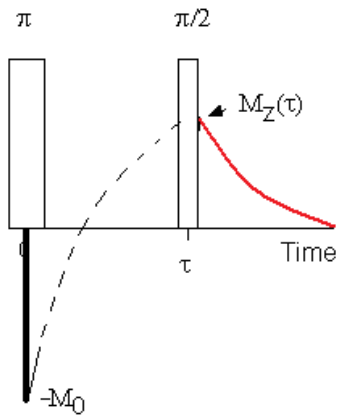

Figure 2.2. *Inversion recovery pulse sequence. The initial magnetization M_0 directed along the positive z-axis (static magnetic field direction) is inverted by a π-rf-pulse. During time τ the magnetization is growing steadily until a second rf-pulse ($\pi/2$-pulse) is applied for detection.*

For instance, the first rf-pulse will be a 180°-pulse. Immediately after such a pulse M_z will be equal to - M_o and no signal will be detected in the xy-plane ($M_x = M_y = 0$). However, if applying a 90°-puls a time τ after the 180^0-pulse the magnetization in the xy-plane will be different from zero and equal to $M_z(\tau)$.

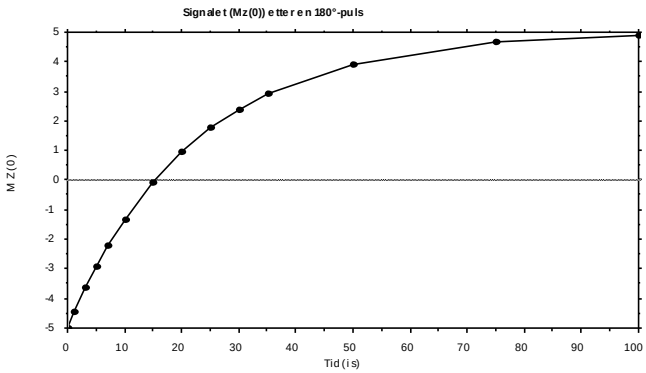

An example showing how $M_z(\tau)$ varies with τ is depicted on Figure 2.3. The points represent ^{13}C-signal intensities from a sample of benzene at room temperature. The solid curve represents a non linear least-squares model fit to the observed data with T_1 equal to 22.5 s.

***Figure 2.3**. Model fitted curve ($M_z = M_o(1\text{-}2\ e^{-\tau/T_1})$) to the observed spin-lattice relaxation data of benzene as obtained by an inversion recovery pulse sequence(Figure 2.2).*

2.3 Molecular dynamics

Generally, a molecular motion can be characterized by some correlation time denoted by τ_C. For instance, the motion of a water molecule may be characterized by a rotational correlation time τ_R (the time needed to rotate one radian) and a translational correlation time τ_T (the time needed to diffuse one radian). We may then define a "memory" function:

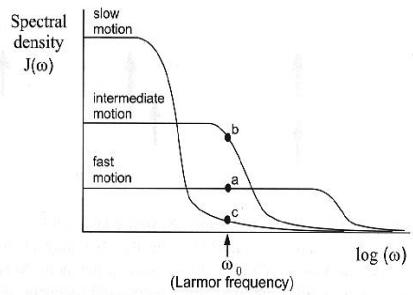

Figure 2.4

$$f_C(\tau) = e^{-\tau/\tau_C} \qquad (2.3)$$

which simply tells us that after a time of the order of $t \approx 5\tau_C$ all motial memory is lost. By fourier transforming Eq 2.3 we obtain the characteristic frequency spectrum $J(\omega)$ of the molecular motion (fluctuations of the internally generated magnetic fields caused by molecular tumbling) which reads:

$$J(\omega) = \int_{-\infty}^{\infty} f_C(\tau) e^{i\omega\tau}\, d\tau = \frac{2\tau_C}{1+\omega^2\tau_C^2} \qquad (2.4)$$

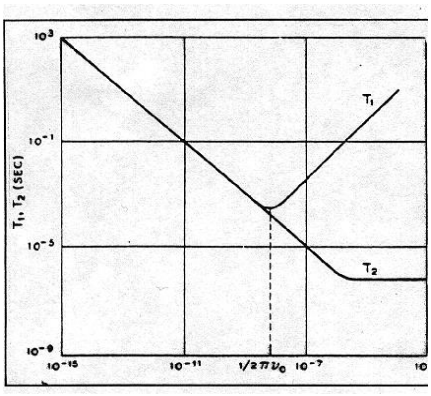

Figure 2.5

The frequency fumction J(ω) is denoted a spectral function in which $dN = J(\omega)d\omega$ simply represents the probability of finding a molecule with a frequency of motion between ω and ω+dω. This function is illustrated in Figure 2.4 for three different values of τ_c (from Claridge 1999) where the inverse of the correlation time $1/\tau_c$ is the jump frequency. The molecular motion results in a fluctuating magnetic field in the position of the spins and will induce transitions between energy levels and thus affect both T_1 and T_2. Figure 2.5 illustrates how T_1 and T_2 depend on the correlation time τ_C; For instance:

$$\frac{1}{T_1} \propto J(\omega) = \frac{2\tau_c}{1+\omega^2\tau_c^2} \qquad (2.5)$$

It is, however, outside the scope of this work to derive Eq 2.5. The graph shows that T_1 goes through a minimum (Exercize 2.4). At the T_1-minimum (Figure 2.5) the jump frequency $1/\tau_c$ can be assigned and is identified with the Larmor frequency, as illustrated by curve b in Figure 2.4. For slower motion (longer τ_C; curve c in Figure 2.4) T_1 will increase while T_2 will decrease and subsequently reach a constant value, the rigid-lattice T_2.(Figure 2.5). For faster motions, T_2 will be equal to T_1 (Figure 2.5) and both relaxation times will will increase with decreasing correlation time (faster motion). Since there is an intimate relation between correlation time and temperetaure (ref. Arrhenius equation), short correlation times are often associated with motions at high temperature. Hence, from Eq 2.5 we notice that at high temperature $(\omega^2\tau^2 << 1)$, T_1 (and T_2) will be independent on the resonance frequency and proportional to τ_C.

2.4 Fourier Transformation (FT)

In practical NMR spectroscopy it is easier to analyze a frequency spectrum F(ω) rather than the time signal f(t), or the fid. The spectrum and the fid contain the same information, but is presented in different ways. It is possible to calculate the one from the other by a mathematical operation called Fourier Transformation.

If we denote the fid by:

$$f(t) = M_0 e^{-t/T_2} e^{-i\omega_0 t} \qquad (2.6)$$

its fourier transform F(ω) can be derived (see Exersice 2.5) and reads:

$$F(\omega) = \int_{-\infty}^{\infty} f(t) e^{i\omega \cdot t} dt = R(\omega) + iI(\omega) \quad ‘$$

$$F(\omega) = \frac{T_2}{1 + ((\omega - \omega_o)T_2)^2} M_0 + i \frac{(\omega - \omega_0)T_2^2}{1 + ((\omega - \omega_0)T_2)^2} M_0 \qquad (2.7)$$

where the real component R(ω) represents the absorption mode (Lorenzian function) and the imaginary component I(ω) represents the dispersion mode, respectively.

The opposite is also true, i.e., the fid is the Fourier transform of the (frequency) spectrum:

$$f(t) = \int_{-\infty}^{\infty} F(\omega) e^{-i\omega \cdot t} d\omega = M_0 e^{-t/T_2} \qquad (2.8)$$

We notice from the real part R(ω) of the spectrum (Eq 2.7) that the width (Δ) at half height is related to the decay rate $1/T_2$ of the fid, i.e., $\Delta = 1/\pi T_2$. When T_2 is short, the fid will decay fast and the frequency peak will become broad.

The FT is quickly performed using a dedicated computer. In principle the relation between the fid and the frequency spectrum has been known from the early days of NMR. However, it was first when computers got cheap enough that it became advantageous to transform the fid by FT.

It is important to know that actually two time-signals, differing in phase by 90^o, are sampled and that the two spectra are mixed in an operation called phasing in order to obtain a pure absorption spectrum.

Because a computer is a digital sampling device, it is necessary to chop the fid. This is done in an analogue-to-digital converter. After the fid has been digitized, the fid consists of a series of points. It is necessary to select a sufficiently large number of points to get the shape sufficiently accurate. A least 4 points are needed to define a peak. On the other hand: the calculating time increases with the number of points. To make the calculation faster the number of points is always 2^n (with n being an integer). In MRI one frequently apply 512 (n = 9) data points. In MR-spectroscopy the number of points is often set to 16384 (n=14). It is also possible to use other tricks to improve the quality of the spectrum, for instance by filtering or selective weighting of parts of the fid before FT.

2.5 Signal-to-noise

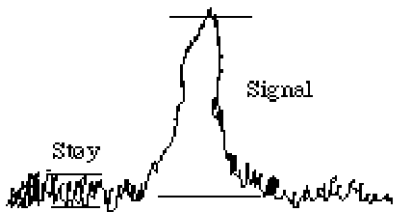

Figure 2.6

MR is not very sensitive compared to other spectroscopic techniques. This is due to the fact the energy of a photon is small compared to kT, making the difference between the numbers of spins in the two energy levels small, which in turn results in a weak signal (see Eq 1.8). However, in one respect this is an advantage. The amount of energy absorbed by the sample will be so small that it will not significantly affect the sample temperature. This is in contrast to other

spectroscopic methods where the irradiation may substantially heat the sample. A number of methods have been introduced to increase the signal-to-noise ratio in the MR-spectrum (see the figure where *støy* stands for *noise*). A closer analyses shows that the S/N-ratio is given by the following expression (Claridge 1999):

$$\text{S/N-ratio} = (\text{number of spins})\text{x}(\text{Abundance})\text{x}(\text{number of fids})^{1/2}\frac{\gamma^{5/2}B_o^{3/2}T_2^*}{T} \qquad (2.9)$$

A simple method to increase S/N is thus to sum the fids after acquiring a larger number of individual fids. After each fid the digitized fid is stored in the computer. The stored signal will increase proportional to the number of fids, while the (random) noise will only increase as the square root of the number of fids. The S/N-ratio therefore increases with the square root of the number of fids. For instance, the S/N-ratio after 100 pulses will be enhanced by a factor of 10.

This increase in the S/N-ratio implicitly assumes that the spin system returns to equilibrium between each rf-pulse and implies that the time between each pulse must be set to approximately 5 times the T_1. If this condition is satisfied the spectrum can be used for quantitative analysis as each peak in the spectrum will be proportional to the number of spins contributing to that peak. If the spectrum is needed to be recorded faster, a closer analysis shows that the best S/N-ratio is obtained by pulsing as fast as possible with a pulse angle shorter than 90^o. However, this approach will introduce systematic errors. Since T_1 may be different for different peaks in the spectrum, peaks with the longest T_1 will be systematically smaller.

2.6 Exercises

2.1) Set up the general Bloch equation in the rotating frame of reference. Write down the Bloch equation when on resonance ($\omega = \omega_0$)

2.2) Assume that you have applied a B_1 field such that $M_y(0) = M_0$, $M_x(0) = 0$ and $Mz(0) = 0$ in the laboratory frame. Set up the Bloch equation (in the rotating frame) and find the solution for $M_y(t)$ and $M_z(t)$ when $\omega_1 = 0$ (B_1 field is turned off) and you are "on resonance". Explain this experiment.

2.3) You want to perform an Inversion Recovery experiment. Set up the Bloch equation (in the rotating frame of reference) and show that the final result is equivalent to Eq 2.2 with $\cos\alpha = -1$. Consider only the z-component (M_z)

2.4) Show that T_1 goes through a minimum when increasing the correlation time (decreasing the temperature). (Hint: use Eq 2.5)

2.5) What is the frequency spectrum $F(\omega)$ of the transversal magnetization $M_y(t)$ in Exercise 2.2

2.6) Set up the Bloch equation in the rotating frame of reference ($\omega = \omega_0$) when a static gradient field $\mathbf{G} = g_0 z\mathbf{k}$ is present along the external magnetic field B_0 (z-axis). Assume $B_1 = 0$

2.7) If denoting the number of spins in the two possible energy levels of a spin-½ system by N^+ and N^-, and we introduce the so called transition probabilities W^+ and W^- (W^+ defines the probability for a spin going from the lower to the higher energy level and W^- represents the probability for a spin going from the higher to the lower energy level) we can set up an equation for how the population difference ($\Delta N = N^+ - N^-$) varies with time: Show that: $\frac{d(\Delta N)}{dt} = -(W^+ + W^-)\cdot(\Delta N - \Delta N_0)$

What is the meaning of ΔN_0 ?
Actually, the spin-lattice relaxation rate $1/T_1$ is defined by $1/T_1 = W^+ + W^-$.
Show that this leads to the famous result: $\frac{dM_z}{dt} = -\frac{M_z - M_0}{T_1}$

3. Spin-echo and diffusion

3.1 Local magnetic fields

The magnetic field in the position of a spin is determined by the sum of the external magnetic field B_o and the local magnetic field B_{lok}. There will be different types of local fields, some intrinsic to the sample, and some which may be more or less controlled. Some local fields shift the peaks in the spectrum while others are responsible for additional fine structures. As a consequence, the information obtainable from a MR-signal depends on how successful these shifts and fine structures can be detected and analyzed.

3.2 Spin echo

The MR-signal originates from that part of the sample which is located within the receiver coil. Ideally, the external magnetic field does not vary over the sample volume. However, this is not the case in practise. In the real world the magnetic field will vary from one place in the sample to another.
This variation in magnetic field over the sample volume is called inhomogeneity and may be reduced by shimming. All MR-magnets are equipped with (correction) coils. When a current is introduced in these coils they set up magnetic fields which may partly counteract and hence reduce the inhomogeneities within the sample volume. How constant the resulting magnetic field will be depends on the size of the sample and the skills of the operator.

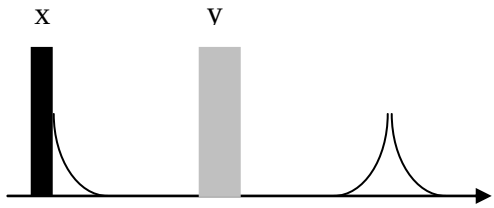

Figure 3.1

In all modern MR spectrometers, this shimming may be performed automatically within a reasonable time. For a liquid sample the width of the resonance peaks are generally determined by the residual magnetic field inhomogenities and implies that the experimentally determined T_2 (from the fid) is shorter than the real and inherent T_2. The former is therefore usually denoted T_2*.

The true T_2 can be determined in an ingenious way by applying a series of rf-pulses in series. If we first apply a 90°-pulse and then, after a time τ, irradiate the sample with a 180°-puls, a signal will appear after a further time τ, as illustrated in Figures 3.1 and 3.2. **(**The first rf–pulse is applied along the x axis and the second rf-pulse is applied along the y axis).

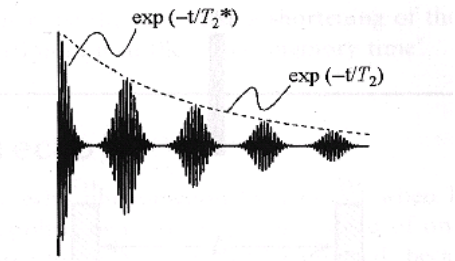

Figure 3.2

The signal, which consists of two fids, is called an echo. We can apply a series of 180°-pulses with a time separation 2τ. Between each 180^{o}-pulses an echo is formed. The envelope of these echoes will be an exponential function with time constant T_2, as shown in Figure 3.2 (from Freeman, 2003). The actual pulse sequence is called a CPMG pulse sequence after the people who developed it,Carr, Purcell, Meibom and Gill.
Actually, the appearance of an echo was first observed and reported by Erwin Hahn around 1950. An important property of the echo, utilized in MRI, is that it appears far from the transmitter pulse in the time domain. The echo is much stronger than the fid, because the latter is not observable during the time when the receiver is turned off. The receiver is blanked for a few micro seconds to avoid break through of the transmitter pulse.

We will now explain why an echo appears. To make it simple we will assume that the local magetic field only has two values $\pm$ b. M is then the sum of two components. After a 90°-pulse about they-axis M is located along the x-axis.

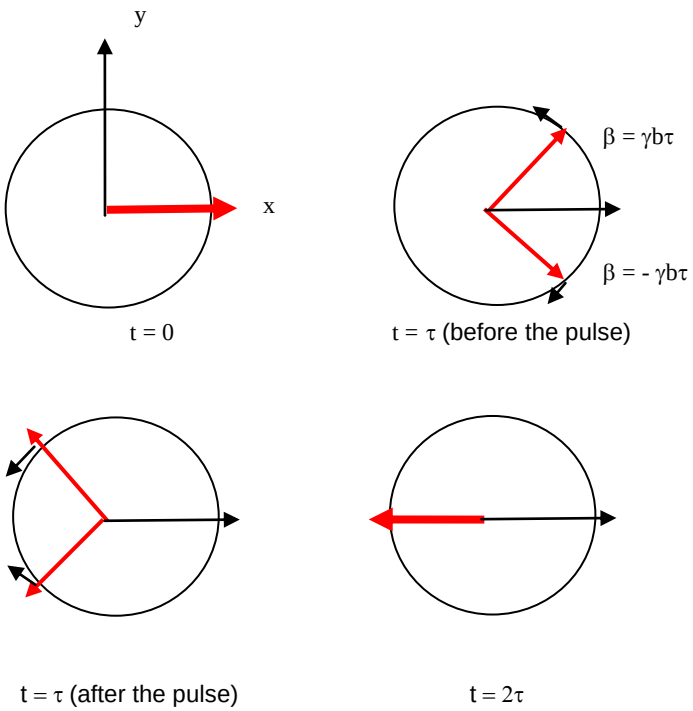

Figure. 3.3. Illustration of the spin-echo experiment. After the magnetization is rotated into the xy-plane by a 90^{0}-pulse (around the y-axis), it looses phase coherence (due to inherent T_2-effects and/or magnetic field inhomogeneities) and is exemplified by the formation of different local magnetic fields ($\pm$b), which in turn causes the spins to presses with slightly different frequencies.

After a time τ the faster rotating component will have dephased an angle + β (= $\gamma b\tau$) while the other component will have moved an angle - β. If we now apply a 180°-pulse to the spin system about the y-axis, the component that rotates faster will make an angle $-\beta$ with the y-axis after the pulse, while the one that rotates slower will make an angle $+\beta$ with the y-axis. However, since they both have the same angular velocity they will both be located along the y-axis after a further time τ and will thus generate an echo.

If we assume a normal distribution of local magnetic fields, M will consist of a continuum of components. After the 90^o-pulse the components will be spread out in the xy-plane. As the fid is a measure of this spread, the fid will die out with a time constant of T_2^*. If we after a time τ ($>T_2^*$ but $<T_2$) apply an 180^o-pulse we will get a situation where the fastest components suddenly are lagging behind and the slower components are ahead. Since they still rotate with the same speed as before the pulse, they will again meet at the y-axis after time τ (echo). The actual reduction in signal intensity of the echo is due to the inherent and true T_2-processes.

This pulse experiment may be compared to a track-race, i.e., before start the runners are all positioned on the same line. After start they will spread out because they run at different speeds. If the starter fires again, and everybody has to turn and run in the opposite direction, at their earlier speeds, they will cross the start line simultaneously.

If some of the runners change speed or give up, the number of runners coming back to the start line at the same time will be reduced.

It follows from this explanation that the echo will consist of two fids (as shown in Figure 3.2); one fid building up to an echo maximum, and the other fid decaying from the time of the echo maximum.

An advantage with the echo technique is that the complete fid is observed. The fid observed immediately after an rf-pulse is truncated because the receiver is turned off during the rf-pulse and for a short time afterwards (to circumevent breaktrhroughof the rf-pulse). The time between the end of the transmitter pulse and the opening of the receiver is called the dead time. The echo on the other hand, is recorded in a situation where the transmitter has been turned off for a long time. It is therefore an advantage to use the echo and not the initial fid in situations where T_2 is short. This is used in whole body MRI where the magnetic field is fairly inhomogeneous.

3.3 Diffusion.

The equation describing the time (t) and spatial (z) dependence of the transversal magnetization $\hat{M}\ (= M_x + iM_y)$ during diffusion, normal to this plane reads (see Excersice 3.1):

$$\frac{\partial \hat{M}}{\partial t} = -i\gamma z g \hat{M} - \frac{\hat{M}}{T_2} + D\nabla^2 \hat{M} \qquad (3.1)$$

$$with\ ; \quad \hat{M} = M_x + iM_y$$

where D is the diffusion coefficient and $1/T_2$ is the spin-spin relaxation rate.
After some complex and elaborate calculations using inverse Laplace transformation R.F. Karlicek and I.J. Lowe presented a solution to this equation:

$$\hat{M}(2\tau) = \hat{M}_0 \exp\left[-t/T_2 - \gamma^2 D \int_0^{2\tau} \left(\int_0^{t'} g(t'')dt''\right)^2 dt'\right] \qquad (3.2)$$

In Excercises 3.2 and 3.3 we justify that Eq 3.2 actually represents a solution to Eq 3.1 where $\hat{M}(2\tau)$ is the signal amplitude at the echo maximum. In particular, we note that the z-parameter is eliminated in Eq 3.2 (see Exercise 3.2). We will in the next section illustrate the applicability of Eq 3.2.

3.4 Spin-echo in a constant magnetic field gradient

The pulse sequence applied is illustrated on Figure 3.4 with g =G_0 representing a constant gradient field across the sample.

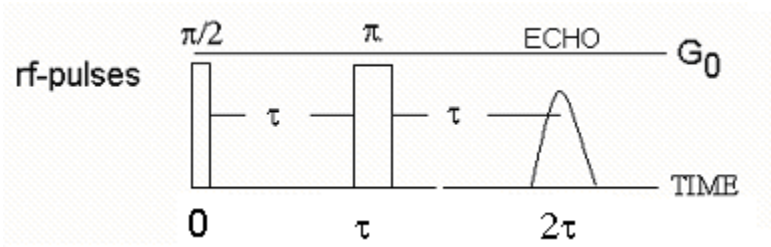

Figure 3.4 *Spin-echo pulse sequence performed in a static magnetic field gradient g = G_0 where τ is the time at which a $\pi/2$-pulse is applied with a subsequent occurence of an echo at time 2τ.*

Before applying Eq. 3.2, we note that in a rotating frame of reference (on resonance), the integral term $z_0\gamma\int_0^{t'} g(t'')dt''$ represents the phase of the magnetization at time t', at position z_0. Without loss of generality we may set z_0 = 1, which implies that the integral $g(t') = \gamma\int_0^{t'} g(t'')dt''$ in Eq 3.2 is identical to (or proportional to) the phase angle. Figure 3.5 illustrates how this phase angle changes during time when applying the pulse sequence in Figure 3.4. Again,

assuming on resonance conditions and describing the phase abgle in the rotating frame of reference we can easily determine the phase angle as a function of time (Figure 3.6) by referring to Figure 3.5.

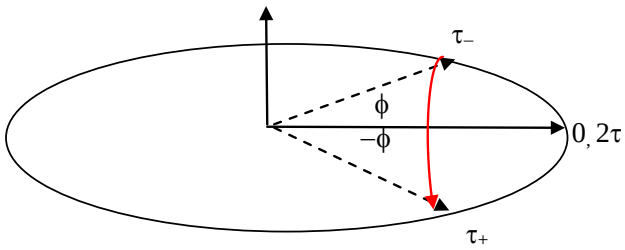

Figure 3.5. Phase angle as a function time when applying the pulse sequence shown in Figure 3.4.

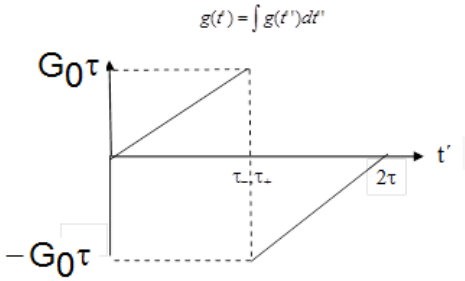

Figure 3.6. Schematic view of the phase angle g(t') as a function of time (t') when applying the pulse sequence shown in Figure 3.4.

A more detailed numerical analysis is shown in the Table 3.1.

Table 3.1. Derivation of the phase term $g(t') = \int g(t'')dt''$ as a function of time t' by referring to Figures 3.5 and 3.6.

Time interval nr. (i)	Time interval	Gradient g(t'')	$g_i(t') = \int_0^{t'} g(t'')dt''$	$(\int_0^{t'} g(t'')dt'')^2$
1	$t_1 = 0$, $t_2 = \tau$ $(= \tau_-)$	G_0	$G_0 t'$	$G_0^2 t'^2$
2	$t_2 = \tau$ $(= \tau_+)$ $t_3 = 2\tau$	G_0	$= G_0 (t' - 2\tau)$	$G_0^2 (t' - 2\tau)^2$

We can now easily calculate the last exponential term in Eq. 3.2 by insertion, i.e.:

$$-\int_0^{2\tau}(\int_0^{t'} g(t'')dt'')^2 dt' = -\int_0^{\tau}(\int_0^{t'} g(t'')dt'')^2 dt' - \int_{\tau}^{2\tau}(\int_0^{t'} g(t'')dt'')^2 dt' \qquad (3.1)$$

$$= -G_0^2 \cdot \left[t'^3/3\,\Big|_0^{\tau} + (t' - 2\tau)^3/3)\,\Big|_{\tau}^{2\tau}\right] = -2G_0^2\tau^3/3$$

The first echo intensity will thus have the intensity;

$$\frac{I(2\tau)}{I(0)} = \exp(-2\tau / T_2 - 2DG_0^2\gamma^2\tau^3/3) \quad (3.2)$$

Likewise, the n'th echo intensity reads:

$$\frac{I((n+1)\cdot 2\tau)}{I(n\cdot 2\tau)} = \exp(-2\tau / T_2 - 2DG_0^2\gamma^2\tau^3/3) \quad (3.3)$$

It follows from Eq 3.3 that:

$$\frac{I(n\cdot 2\tau)}{I(0)} = \frac{I(t)}{I(0)} = \prod_n \exp(-2\tau / T_2 - 2DG_0^2\gamma^2\tau^3/3) \quad (3.4)$$
$$= \exp(-n\cdot 2\tau / T_2 - 2DG_0^2\gamma^2 n\cdot\tau^3/3) = \exp\left[-t(1/T_2 + DG_0^2\gamma^2\tau^2/3)\right]$$

3. 5 Example.

3.5.1. Diffusion in bulk water.

Figure 3.7 (left) shows the signal intensity of bulk water for different diffusion times t_D as a function of the gradient field strength squared (g^2). The dotted curves represent non linear least squares fit to Eq 3.4. The derived diffusivity as a function of diffusion time is plotted on Figure 3.7 (right) and suggests that for bulk water the diffusivity is independent on diffusion time and equals $(2.58 \pm 0.08)\cdot 10^{-9}$ m^2/s[18].

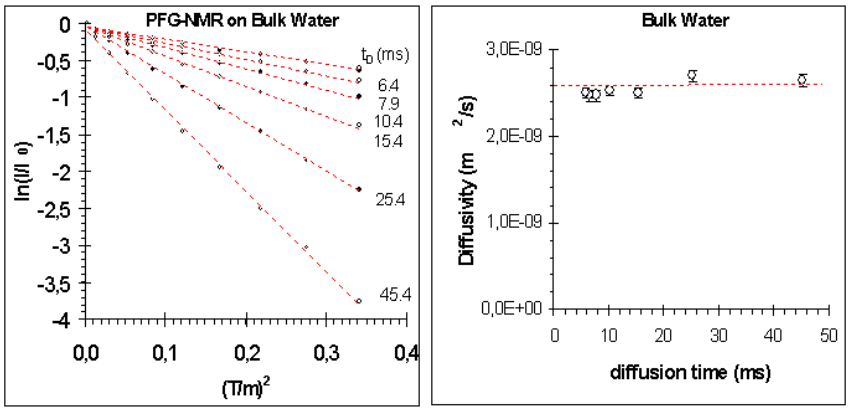

Figure 3.7. *Left: Observed echo intensity (normalized) of bulk water as a function of diffusion time (t_D) and the gradient field strength squared g^2. Right: Bulk water diffusivity as a function of diffusion time.*

3.5.2 Diffusion of bulk water within pores.

For distilled water containing no oxygen, the relaxation times T_1 and T_2 are expected to be identical. However, for bulk water confined in a porous matrix the spin-spin relaxation rate $1/T_2$ depends on the inter-pulse time 2τ (Figure 3.9A) in much the same way as observed for bulk water in a static gradient field, as discussed in the last section.

---

[18] Hansen, E.W and coworkers, Microporous and mesoporous Materials, **2005**, 78, 43-52.

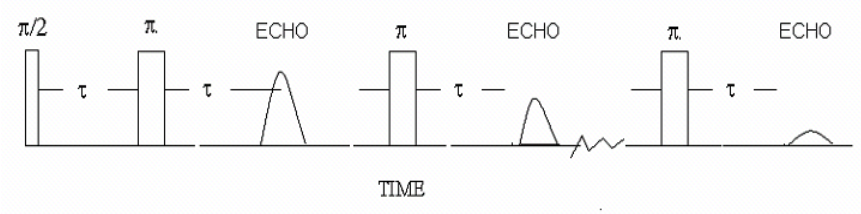

Figure 3.8. A train of spin-echo pulses illustrating the Carr-Purcell-Meiboom-Gill-pulse sequence (CPMG)**.**

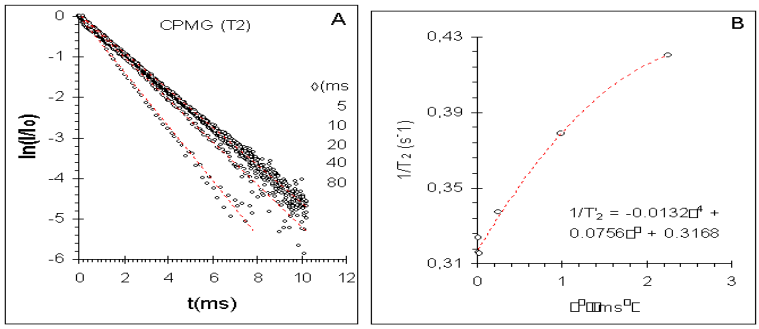

Figure3.9 A) *The echo signal intensity of bulk water as obtained from a CPMG pulse train with different time distances (2τ) between successive π-pulses. The solid curves represent non-linear least squares fits to a single exponential function M =exp(-t/T'$_2$).* ***B)*** *The apparent spin-spin relaxation rate (1/T`$_2$) versus τ^2. The true spin-spin relaxation rate (1/T$_2$) is determined from a second order polynomial fit in τ^2 at $\tau = 0$, resulting in T$_2$ = (3156 ± 50) ms.*

Actually, the observed relaxation rate $1/T_2$ of the pore confined water shows the same quadratic τ-dependence as for water diffusing in a constant gradient field (Figure 3.9B, Eq 3.4) suggesting that a gradient field exist across the sample volume is formed. We tentatively believe that this gradient magnetic field originates from a discontinuity of the magnetic field lines at the interface between the solid matrix (glass beads) and the (pore confined) water or/and due to a inhomogeneous external magnetic field B_0.

The dotted (red) curve in Figure 3.9B represents a non-linear least squares fit to a second order polynomial in τ^2 and explains semi-quantitatively the experimental data. The true T_2 is derived from the intercept of this curve with $\tau = 0$ and reads T_2 = (3156 ± 50) ms, showing that $T_1 \approx T_2$, as expected for bulk water.

3.6 Spin-echo in a pulsed magnetic field gradient.

Let us return to a more complex pulse sequence shown in Figure 3.10. Using the

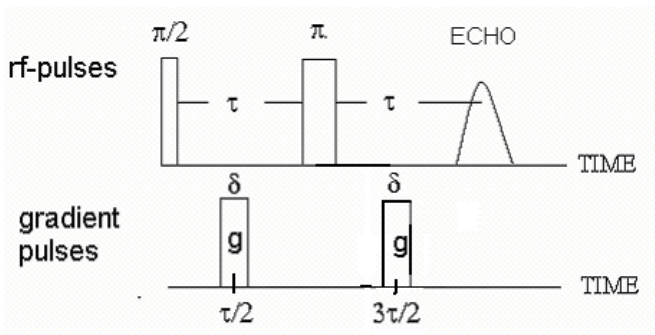

Figure 3.10. *Illustration of the simplest pulsed field gradient pulse sequence used to measure diffusivity. g represents the strength of the pulsed gradient field of duration δ. The timing of both rf-pulses and gradient pulses is shown along the time axis.*

same approach as outlined in section 3.2.1 the phase angle $g(t') = \gamma \int_0^{t'} g(t'')dt''$ as a function of time t' can easily be derived (Figure 3.11). A more quantitative numerical analysis is shown in Table 3.2

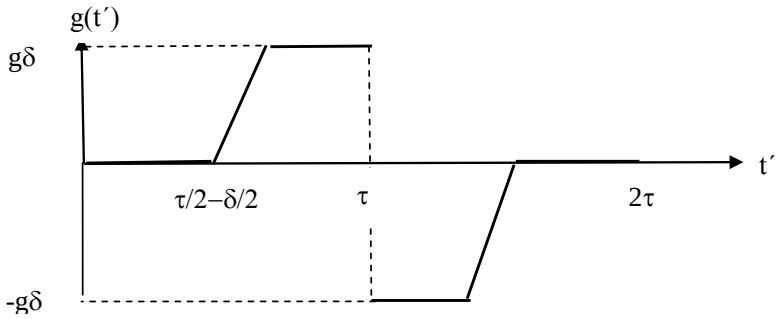

Figure 3.11. Illustration of the phase angle g(t') as a function of time t' when applying the pulse sequence shown in Figure 3.10.

Table 3.2. Effective gradients and integrals[1)]

Time interval nr. (i)	Time interval	G(t'')	$g_i(t') = \int_0^{t'} g(t'')dt''$	$(\int_0^{t'} g(t'')dt'')^2$
1	t_1=0, t_2=τ/2–δ/2	0	0	0
2	t_2= τ/2–δ/2, t_3=τ/2+δ/2	G	$gt' - g(\tau-\delta)/2$	$[gt' - g(\tau-\delta)/2]^2$
3	t_3 =τ/2+δ/2, t_4=τ	0	$g\delta$	$g^2\delta^2$
4	t_4 =τ, t_5=3τ/2–δ/2	0	$-g\delta$	$g^2\delta^2$
5	t_5 =3τ/2–δ/2, t_6=3τ/2+δ/2	G	=gt´- g(3τ+δ)/2	=[gt´- g(3τ+δ)/2]^2
6	t_6 =3τ/2+δ/2, t_7=2τ	0	0	0

[1)]Generally we have that: $g_i(t') = at' + b$ where a = 0 or ± g, depending on whether the gradient is on or off. The parameter b is determined from the continuity at the various intersection ponts.

We can then easily calculate the integral $\int_0^{2\tau} (\int_0^{t'} g(t'')dt'')^2 dt'$ as follows:

$$\int_0^{2\tau}\left(\int_0^{t'} g(t'')dt''\right)^2 dt' = (g^2/3)\left[\left[t_3 - (\tau-\delta)/2\right]^3 - \left[t_2 - (\tau-\delta)/2\right]^3\right] + g^2\delta^2(t_5 - t_3)$$
$$+ (g^2/3)\left[\left[t_6 - (3\tau+\delta)/2\right]^3 - \left[t_5 - (3\tau+\delta)/2\right]^3\right] \qquad (3.5)$$
$$= g^2\delta^3/3 + g^2\delta^2(\tau-\delta) + g^2\delta^3/3$$
$$= g^2\delta^2(\tau - \delta/3)$$

Hence, from Eq 3.2:

$$\frac{M(2\tau)}{M(0)} = \exp\left[-t/T_2 - \gamma^2 D\int_0^{2\tau}\left(\int_0^{t'} g(t'')dt''\right)^2 dt'\right] \qquad (3.6)$$
$$= \exp\left[-t/T_2\right]\cdot\exp\left[-\gamma^2 g^2\delta^2(\tau - \delta/3)\cdot D\right]$$

3. 7 Tomography

We have seen that the width of a liquid-peak in a MR-spectrum is determined by the inhomogeneity in the external magnetic field. Inhomogenity means that the field varies from one point to another in space and is unwanted in MR spectroscopy. However, it may be turned into something very useful. If introducing a magnetic field that varies across the sample, we can observe a signal from a restricted part of the sample. The basic equation tells us that if we apply an rf-pulse of frequency ν then only the spins in the magnetic field B (= $2\pi\ \nu\ /\gamma$) will be irradiated and contribute to a signal. The simplest case is to let the added magnetic field increase linearly in one direction (x), $B = B_o + xG_x$, i.e., a constant gradient field along the x-axis.

The upper figure show two capillaries filled with ordinary water in a test tube containing heavy water. We note that the observed MR-spectrum depends of the direction of the gradient. Each spectrum is a projection of the sample along the direction of the gradient. From a set of such spectra it is possible to construct an image of the sample.

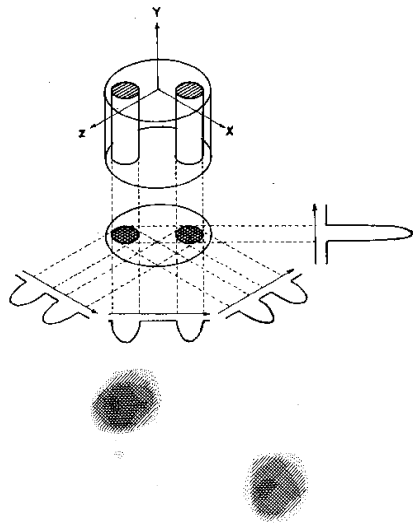

The lower figure show the picture constructed from these spectra and represents the first MR-picture published in the literature.[19] A more detailed outline of this technique will be addressed in the second part of this course.

Field gradients are also used in MR-spectroscopy to measure diffusion, as discussed in a previous section. Also, in ordinary solution NMR spectroscopy the application of gradient fields is found to be of significant advantage (see Claridge 1999).

[19]Lauterbur in Nature 242(1973)190

3.8 Exercises

3.1) You apply a gradient field ($\vec{g} = g_0 \cdot z\vec{k}$) along the z-axis which is parallel to the external magnetic field $\vec{B}(= B_0\vec{k})$ B. If applying the Bloch equation, show that the transversal magnetization, i.e., the complex magnetization $\hat{M}$ ($\hat{M} = M_x + iM_y$), satisfies the following relation; $\frac{\partial \hat{M}}{\partial t} = -i\gamma g_0 z\hat{M} - \frac{\hat{M}}{T_2} + D\frac{\partial^2 \hat{M}}{\partial z^2}$

3.2) Show that a general solution to the above equation can be written:

$\hat{M}(z,t) = e^{-t/T_2}\hat{m}(z,t)$ *with* $\frac{\partial \hat{m}}{\partial t} = -i\gamma g_0 z\hat{m} + D\frac{\partial^2 \hat{m}}{\partial z^2}$

3.3) If introducing the following trial function: $\hat{m} = \psi(t)\cdot\exp\left[-i\gamma z\int_0^t g_0(t')dt'\right]$

Solve for ψ(t) and argue that this function actually describes the echo attenuation in a Pulsed Field Gradien Spin Echo experiment, i.e.; $\psi(t) = \psi(0)\cdot\exp\left[-\gamma^2 D\int_0^t\left(\int_0^{t'} g(t'')dt''\right)^2 dt'\right]$

3.4) Go through sections 3.4 and 3.6 on your own and perform all calculations.

4. Shielding and coupling

4.1 Chemical shift

All atoms in a molecule are surrounded by electrons which bind the atoms together. The electron distribution can be regarded as a charged cloud. When such an electron cloud is placed in a magnetic field B_0 a current will be induced which in turn generates a local magnetic field B_{loc} (according to Lenz' law this magnetic field will oppose the static magnetic field B_0). We say that the electron cloud *shields* the spins. When the cloud has spherical symmetry this induced field will be directly proportional to the external field ($B_{loc} = -\sigma B_0$) .The proportionality factor σ is called the shielding constant and the actual magnetic field sensed by any nucleus may be expressed by:

$$B = B_0 + B_{loc} = (1-\sigma)B_0 \qquad (4.1)$$

which can be rewritten in the form form:

$$\omega = \gamma(1-\sigma)B_0 \qquad (4.2)$$

In a molecule or ion the shielding constant will vary from one spin to another if they are chemically different.

For example in ethanol (CH_3CH_2OH) - the electric cloud around the methyl carbon (CH_3-) is different from the electric cloud around the methylene carbon (-CH_2-).

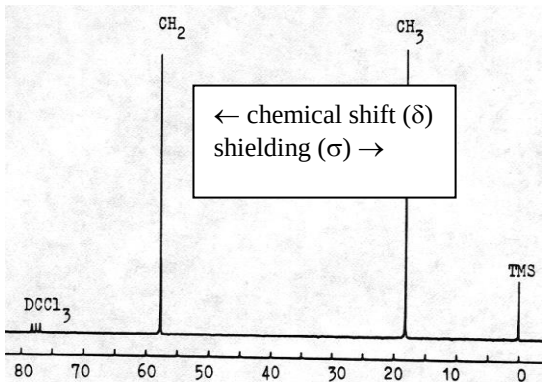

Figure 4.1

The ^{13}C-MR spectrum of ethanol therefore Is expected to consist of two peaks with resonance frequency ν_1 and ν_2 (plus three small peaks from the solvent (deuterated chloroform ($DCCl_3$)) as shown in Figure 4.1. Using Eq 4.2, the frequency difference between the two peaks can be written:

$$\nu_1 - \nu_2 = (\sigma_2 - \sigma_1)\,\nu_o \text{ where } \nu_o = \gamma B_0/2\pi \qquad (4.3)$$

We see that the frequency difference is proportional to the frequency ν_0 of the spectrometer. To be able to compare data recorded in spectrometers with different magnetic fields a dimensionless parameter denoted the chemical shift δ was introduced:

$$\delta = \frac{\nu_1 - \nu_2}{\nu_o}(\nu_o \text{ i MHz}) \qquad (4.4)$$

It is common practise to measure the chemical shift relative to a peak in a reference compound. For ^{1}H- and ^{13}C, this reference compound is tetramethyl silane (TMS; $(CH_3)_4Si$) as indicated on the spectrum in Figure 4.1. In TMS the spins are well shielded so the peak does not generally interfere with the peaks from common organic molecules.

Conventionally the TMS-peak is to the right in the spectrum and the δ axis increases to the left. In our example, δ for the methyl carbon is 18.0 ppm and for the methylene carbon 57.3 ppm. The shift difference in frequency units in the magnetic field applied is (4.7 T; 200 MHz for ^{1}H) is ca 2 kHz ((57.3-18.0)x50).

For a solid, the chemical shift is described by a tensor. However, for a liquid the tensor is

averaged to a scalar. The shielding tensor is analogous to the moment of inertia of a body. It is possible to find a coordinate system where all off diagonal elements are zero and the sum of the diagonal elements is zero. The shielding tensor may therefore be uniquely characterized by by two parameters: σ_z and the asymmetry factor η (the largest of the diagonal elements is chosen to be σ_z) and η is a number between 0 and 1:

$$\eta = (\sigma_x - \sigma_y)/\sigma_z. \qquad (4.5)$$

4.2 Indirect spin-spin coupling (J coupling) – 1. order spectral analysis

In the ^{13}C-MR spectrum of ethanol (Figure 4.1) all interactions between the protons and the carbon are removed by what is called ^{1}H-decoupling. However, if these interactions are not removed, the ^{13}C-MR spectrum looks quite different. For instance, Figure 4.2 shows the ^{13}C spectrum of the -CH_2- group in ethanol (the scale is 30 Hz/division).

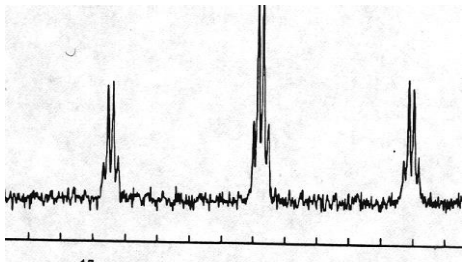

Figure 4.2

and demonstrates that the single peak from the -CH_2- carbon (Figure 4.1) is split up in triplets of quartets. It can be shown theoretically (see next section) that this appearance of fine structure in the spectrum originates from an interaction between the proton spins and the carbon spins. This fine structure of the carbon resonance in methylene can be simply explained by the following arguments: In the methylene group (- CH_2-) there are two ^{1}H-spins directly bonded to the ^{13}C nucleus. Each of these proton spins can take two orientations with respect to the external field, up (↑) or down (↓). For <u>two</u> ^{1}H-spins there are four combinations of spin orientations:

(↑↑)
(↓↑ and ↑↓)
(↓↓)

These different proton spin orientations generate different local magnetic fields at the ^{13}C nucleus and give rise to a triplet peak with an intensity distribution 1:2:1. In addition, the methylene carbon is also coupled to three ^{1}H-spins located on the methyl group (-CH_3). By a similar reasoning, as for the coupling to two ^{1}H-spins, we obtain the following four different spin-orientations of a three-proton-spin system:

(↑↑↑)
(↓↑↑ and ↑↓↑ and ↑↑↓)
(↓↓↑ and ↓↑↓ and ↑↓↓)
(↓↓↓)

Since these four different proton spin-orientations generate different local magnetic fields at the metylene carbon, the latter is further split into four peaks (quartet). The conclusion is that when the protons are not decoupled they split the methylene carbon peak into a triplet, which in turn is split into a quartet.

We can generalise these findings to what is called the “(n+1)”-rule. When a spin-1/2 nucleus is coupled to n equivalent spin-1/2 nuclei, the resonance peak of the former is split up in (n+1)-peaks with an binominal intensity distribution (1:1, 1:2:1, 1:3:3:1,

1:4:6:4:1 for n = 1, 2, 3, 4,….etc). The distance (Hz) between the resolved peaks define the coupling constant J and it is found to be independent on the external magnetic field strength B_0.
The above simplified spectral analysis is correct as long as the chemical shift difference (δ; in Hz) between the coupled nuclei is larger than the coupling constant J between them. We call such spectra "1. order spectra".

As already pointed out in a previous section, the "n+1"-rule is valid as long as the chemical shift difference δ (Hz) between the nuclei is large compared to the coupling constant J between them, i.e., $\Delta\delta$ (in Hz) >> J. When $\Delta\delta$ (in Hz) ≈ J, the intensity distribution of the peaks will not be as predicted by the "n+1"-rule. The positions of the peaks are changed and the multiplet may contain additional peaks. The general analysis of MR spectra necessitates a rigorous quantum mechanica approach and is shown in Appendix B for a two-spin system (two interacting nuclei).

Generally, the coupling constant J is ordered after how many chemical bonds there are between the coupled spins. In the above example, the coupling between the methylene carbon and protons is a one bond coupling of size 120 Hz. The two-bond coupling between the methylene carbon and the methyl proton is smaller, approximately 4 Hz.

One may ask why we do not see a coupling between the carbon nuclei in the molecule. The answer is that only 1.1% of the carbon atoms (^{13}C) possess a spin while the rest (^{12}C) have no spin (I = 0). The observed carbon peaks are from the 98.9% of the ethanol molecules in which the neighbouring carbon nucleusis ^{12}C [20].

Moreover, why does no coupling show up between the methylene carbon and the –OH proton in ethanol, since the latter nucleus is also located two bonds away from the methylene carbon. This is due to molecular motion, i.e., the proton nucleus on the –OH group is hydrogen bonded to other ethanol molecule and hence may jump (or exchange) quickly between different sites which averages out any chemical shift difference due to coupling[21].

4.3 Molecular structure

A typical MR-spectrum (of a liquid) consists of various peaks grouped in multiplets. The number of multiplets tells us how many functional groups are involved in the molecule. For instance, a ^{1}H-decoupled ^{13}C-spectrum will tell how many different carbon atoms there are in a molecule. If the molecule is symmetric, the spectrum will reveal an analogous symmetry.
For instance, a benzene molecule consists of six carbon atoms, but because the molecule has six-fold symmetry the carbon atoms have the same chemical shift and consequently the spectrum will contain only one peak. If one of the protons is replaced by a Cl-atom the molecule will have mirror symmetry and the spectrum will consist of four peaks, two peaks of intensity "1" and two peaks of intensity "2".
As pointed out previously, the molecular motion may average out chemical shift differences. The molecular symmetry found by MR can therefore be higher than the real symmetry of the molecule.

---

[20] This is true at first sight. If the signal/noise is good small multiplets may be observed symmetrically about the main peaks.

[21] The jump rate depends on traces of acid present and the temperature. In pure 100 % ethanol the coupling to the H atom in the –OH group can be seen at room temperature.

The magnitude of the chemical shift depends on the molecular structure and what functional groups exist and where they are located in the molecule. Through the years a large empirical material has been collected and systematized in different ways, originally in form of tables and collections of typical spectra, recently in the form of computer databanks and data programs. This material can be used in the interpretation of MR-spectra of molecules with unknown structure.

Also, the coupling constants give structural information, mainly how the different atoms or functional groups are connected together to form the molecule. Especially the so called vicinal coupling, that is a three bond coupling. The vicinal coupling in an ethane fragment (-H_2C-CH_2-) epends on the dihedral angle as shown in the graph. The gauche coupling (ø = 60°) is small ca 2 Hz, but the trans-coupling (ø = 180°) is much larger 9 Hz. This variation has been used to determine the confor-mation of molecular rings. The vicinal coupling does not only depend on the dihedral angle, but also on the electronegativity of the substituents. Electronegative substituents will reduce the vicinal coupling constant so the derived coupling constant must be used with caution. The coupling constants have also been systematized and the material is accessible in various data bases.

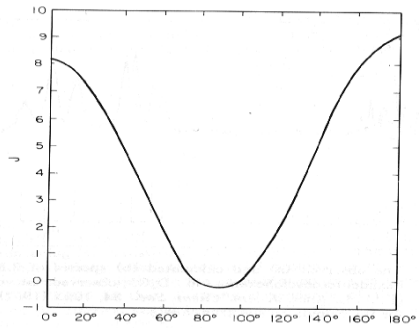

Figure 4.5

In many cases it is rather trivial to interpret MR-spectra to obtain chemical shifts and coupling constants, in particular regarding 1. order spectra. However, when chemical shift differences and coupling constants are of the same order of magnitude, the analysis becomes much more complex and difficult to analyze without sorting to some kind of simulation. Also, use of two dimensional MR may be advanegous, however, this is outside the scope of this course (see Claridge 1999).

4.4 Exercises

4.1) Show that the secular determinant (Eq 4.9b) takes the form:

$$\begin{pmatrix} H_{11}-E & 0 & 0 & 0 \\ 0 & H_{22}-E & H_{23} & 0 \\ 0 & H_{32} & H_{33}-E & 0 \\ 0 & 0 & 0 & H_{44}-E \end{pmatrix}$$

4.2) Why does the secular determinant have the above "form" or "symmetry"?

4.3) From the "structure" of the secular determinant one can immediately conclude that the eigen-functions ψ_2 and ψ_3 are linear combinations of f_2 and f_3. Explain why.

4.4) Solve the secular determinant in Exercise 4.1 and compare your results with the energies (E_i; i = 1-4) presented by Eq 4.9c.

4.5) Calculate the expected resonance frequencies and compare with the results presented in Table 1.

4.6) From quantum mechanical principles, the signal intensity I_{ij} between two eigenstates i and j can be written: $I_{ij} = \gamma^2 (<\psi_i|I_x^1|\psi_j>^2 + <\psi_i|I_x^2|\psi_j>^2)$. Calculate these intensities when knowing that $I_x|\alpha> = 1/2|\beta>$ and $I_x|\beta> = 1/2|\alpha>$. Compare your calculations with the results presented in Table 1.

4.7) Make a sketch of the proton spectra of the following structural fragments and explain your results (use a 1.order approximation).
a) –CHC- **b)** $–CH_2CH-$ **c)** CH_3CH_2- **d)** CH_3CH- **f)** $-CH_3$.

4.8) How will the ^{13}C-NMR spectrum of **b)** and **f)** look like?

5 NMR history

5.1 The development of NMR - Nobel prizes

How did it start? Who has contributed? Did it start in 1925 when two Dutch Ph.D.-students, Uhlenbeck (1900-88) and Goudsmit (1902-78), found fine structure in the optical spectra they studied and explained it by proposing that the electron is a particle with angular momentum and a magnetic dipole moment? Or did it start a year earlier when Wolfgang Pauli (1900-54) proposed that the atomic nuclei had angular momentum. At least it started in 1938 when Isidore Isaac Rabi (1898-1988) used magnetic resonance to improve the accuracy of his measurement. He discovered ^{7}Li- and ^{35}Cl-NMR in LiCl-molecules in the gas phase.

Isidor Isaac Rabi

The experiment was proposed by the Dutch C. J. Gorter (1907-80) when he visited Rabi´s laboratory. Rabi got the Nobel Prize in physics in 1944; Gorter only got acknowledged in the paper Rabi published.[22] This is the first case of many in the history of magnetic resonance. Many contribute, but not more than 3 get a Nobel Prize.
Furthermore it is always the boss who gets the prize not the ones that build the equipment and do the experiments.

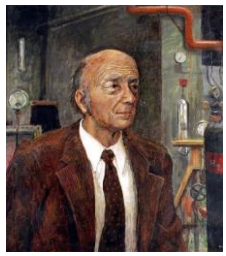

C. J. Gorter

It really started in 1945 when the physicists took up basic research again after the Second World War. Felix Bloch (1905-83) at Stanford and Henry M. Purcell (1912-97) at Harvard discovered independent of each other magnetic resonance in a condensed phase: Bloch in liquid water and Purcell in paraffin wax. They knew that Gorter had tried both before and during the war, but in vain. Afterwards it was found that the T_1 of his samples was too long because his samples F. Bloch were too pure and the temperature was too low**!**

Felix Bloch

Bloch was not interested in magnetic resonance per se, but was looking for a method to measure magnetic field. He used two orthogonal coils and called his method nuclear induction. Due to the brothers Varian, who had earned money on making klystrons during the war, he patented his method and the brothers founded a company that in the early 1950-ties marketed the first commercial NMR spectrometers. What the company Varian continues to do.[23] Bloch published his famous' equations in 1946.[24] Purcell used micro waves in his first measurements. But soon after his colleagues/students built spectrometers using radio equipment.

H.M.Purcell

[22] Rabi et al Phys. Rev. 53(1938)677.
[23] http://www.varianinc.com/cgi-bin/nav?/ The most serious competetor is Bruker-biospin http://www.bruker-biospin.de. Another is Jeol – a jabanese company. Most of the spectrometers presently at the institute are from Bruker, only one older from Varian.
[24] F. Bloch Phys Rev 70(1946)460

Purcell got a Dutch Ph.D.-student, Niels Bloembergen[25], and they developed a simple theory for magnetic relaxation known as BPP after the authors (see Figure 2.5).[26]

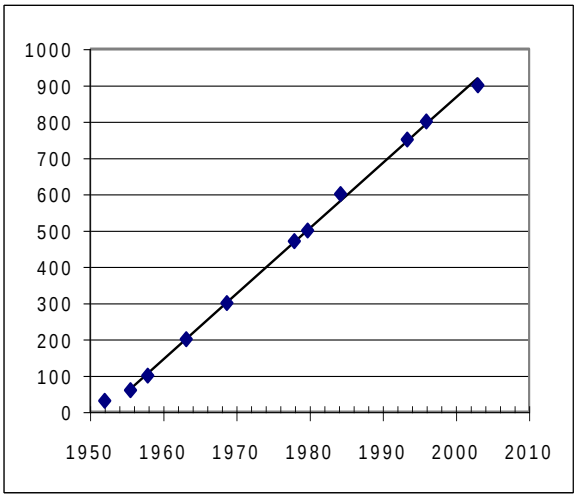

The limitation in the first years after the discovery was not the electronics, but the magnets. They used iron magnets – large heavy beasts The problem was the homogeneity and stability. But when fine structure in the spectra was discovered work to improve the magnet speeded up.

K. Wütrich

In 1948-50 fine structure due to dipole coupling, chemical shift, J-coupling and quadrupole coupling was discovered. Erwin Hahn, Bloch's PhD-student, built the first pulse NMR spectrometer also before 1950 and discovered spin echo. The pulse methods worked even if the homogeneity was bad!

The graph shows the development of magnetic field strength since the first commercial magnets were put on the market in 1952 to the present. The graph is valid for magnets with a gap of 5 cm. Such magnets are used for solution NMR. Maximum field for a commercial magnet to day is 21 Tesla (900 MHz for ^{1}H). If we extrapolate the straight line in the graph we can predict that the 1000 MHz (= 1 GHz) magnet will be put on the market in 2008. Starting from the 200 MHz-magnet all later magnets are not iron magnets but a superconducting coil at 4 K or lower.

The same magnet technology gives a smaller field for a larger gap. In solid state NMR 9 cm gap are used and the maximum field is pt 600 MHz. In MRI for humans the gap is much larger. Commonly a magnetic field of 1.5 T is used, but 3 T magnets are now increasing in number. (3 T corresponds to 128 MHz for ^{1}H).

Higher fields give better sensitivity. That means that the recording time gets shorter or that a good enough spectrum of a smaller amount of sample may be obtained. Also the chemical shift gets higher so the resolution improves. However, high field magnets are expensive. A 900 MHz NMR-spectrometer (figure) costs ca 50 MNOK. There is no such instrument in Norway (but in all the other countries in Scandinavia). One problem with high field magnets is their stray fields and implies that they occupy a lot of space. However, shielded magnets have come available which reduces the required space (but increasescost). With better magnets the electronics became the limiting factor. Transistors replaced radio tubes, and

R. R. Ernst

[25] He was born in 1920 and got the Nobel Prize in physics in 1981 for his contribution to the development of laser spectroscopy.
[26] N. Bloembergen, E.M. Purcell and R.V. Pound Phys Rev 73(1948)986

Integrated circuits were developed.
In the middle of the 1960-ties came the first Digital computers that were cheap enough to be build into a spectrometer. In the 1970-ties the cw-method was replaced by the rf-pulse method. The man who got the honour for this was the Swiss scientist Richard Ernst (1933-), professor at ETH in Zürich. Before this time it was mainly ^{1}H that was studied (at least by chemists). Due to the invention of the rf-pulse technique, natural abundance spectra of Both ^{13}C as well as ^{15}N could be acquired.

P. Lauterbur

Ernst also developed 2D-methods in the 1970-ties. The idea came From The Belgian thermodynamics Jean Jeener, although it was Ernst that did the development work.
These methods made it possible to interpret increasingly more complex spectra of larg molecules.The Swiss scientist Kurt Wütrich (1938-), professor at ETH in Zürich, received one half of the Nobel Prize in 2002 for his development of nuclear magnetic resonance spectroscopy for determining the three-dimensional structure of biological macro-molecules in solution.

Sir. P. Mansfield

Magnetic field gradients were introduced in the 1960-ties to study diffusion and makes the NMR-signal dependent on position.
Paul Lauterbur (1929-) got the idea in 1973, i.e., that a field gradient can applied to image an object, as pointed out in section 3.5. Also, Peter Mansfield (1933-) had the same idea at the same time, but he used pulse methods. In 2003 they sheared the Nobel Prize in medicine for their discoveries Concerning magnetic resonance imaging.
This is a rather short NMR history, covering more than 70 years. For a longer Version, see Grant, 1995. More updated information about the Nobel laureates can be found at http://www.nobel.se/.

5.2 NMR in Norway

The first NMR spectrometer came to Norway in 1960. It was a 60 MHz spectrometer from Varian (picture) placed at SI (now called Sintef-Oslo). It came with all the extra equipment you could buy at that time and could be used for liquids and solids. A pulse spectrometer was also built at SI early in the 1960-ties. The NMR laboratory was closed in 1980, and the activity transferred to the Department of Chemistry at the University of Oslo.

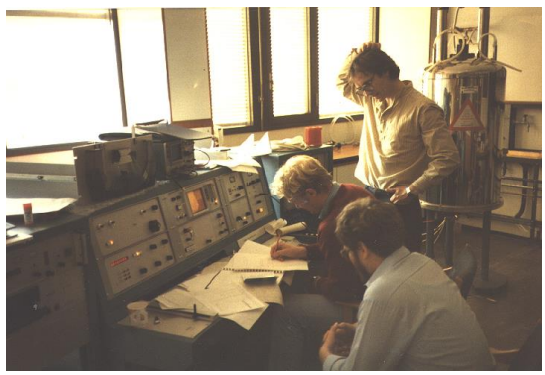

The organic chemists at the Department of Chemistry got the first NMR-spectrometer in 1965 (Varian A-60 shown in the picture). A-60 has now the same status among NMR users as a T-Ford for a car enthusiast. A-60 was made for a mass market as the T-Ford. The A-60 was exchanged with a 100 MHz-

second spectrometer, also from Varian, came in 1970 and was a more advanced, and
complex spectrometer. The first pulse spectrometer with a computer (24 k memory!) came in 1975 (Jeol FT-60), and the first superconducting instrument was bought in 1981 (CPX-200 in 1981 see the picture. The magnet is still in use, but the console is new). In 1989 the organic chemist got a 300 MHz-spectrometer from Varian for solution-NMR. The great year of NMR in Norway was 1995, in which 12 new NMR spectrometers was bought from the German company Bruker and placed in Bergen, Oslo and Trondheim. Oslo got four new spectrometers, 3 for solution NMR (200, 300 and 500 MHz) and a new 200 MHz-consol for solid state NMR.

There is a Laboratory for organic NMR in the east wing wing of the Chemistry Department lead by Frode Rise and Dirk Petersen. They recently got a new 600 MHz-spectrometer which is coupled to a liquid chromatograph (LC) whicn is denoted “LC-NMR”. In the west wing a Laboratory for physical NMR (solid state-NMR) is located and lead by Eddy W. Hansen. Hansen is studying morphological properties, structure and molecular dynamics of solid polymers and also molecular dynamics (diffusion) of liquids in porous solids. They have one low field NMR instrument operating at 22 MHz (Maran Ultra from the British company Resonance). In addition, they have access to a 500 MHz, solid state NMR spectrometer located at Sintef. The two institutions A major collaboration within solid state NMR between the two institutions was established during 2010.

Appendix A. The "13-interval pulse sequence"

When measuring the diffusivity of fluid molecules confined in porous materials the effect of internal gradients, eddy currents (caused by strong gradient pulses) and unwanted echoes (when applying more than a single rf-pulse) must be taken into account. Also, the observation that T_2 is frequently <u>much</u> shorter than T_1 must be considered. This calls for a more complex pulse sequence, the so called "13-interval pulse sequence" (Figure A1). A formula relating the phase angle as a function of time based on the pulse sequence shown in Figure A1 can be derived by implementing the same approach as discussed in the text. However, It is beyond the scope of this course to detail this any further. Actually, we leave this to the interested reader and simply present the final result, Eq A1.

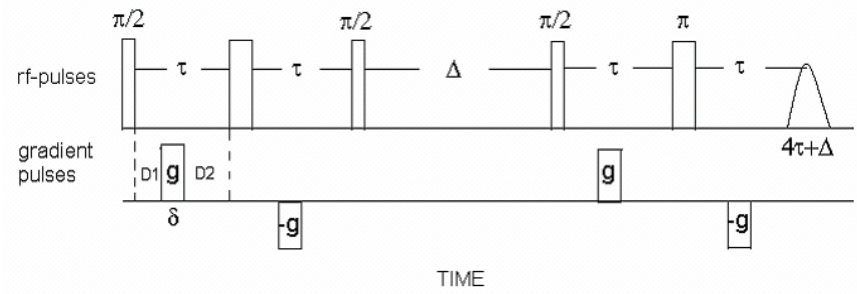

Figure. Illustration of the "13-interval pulse gradient stimulated echo sequence" using bipolar gradients with g representing the strength of the gradient field of duration δ. The timing of both rf-pulses and gradient pulses are illustrated aong the time axis.

$$\frac{M}{M_0} = \exp\left[-\frac{2\tau}{T_2}\right] \cdot \exp\left[-\frac{\Delta}{T_1}\right] \exp\left[-4\gamma^2\delta^2 g^2 D(t_D) t_D\right] \qquad \text{(A1)}$$

$$t_D = \Delta + 3\tau/2 - \delta/6$$

The above equation shows that the self diffusion (D) of a pore confined fluid depends on the diffusion time t_D and is in contrast to a bulk solution, in which D is independent on t_D. Due to the spatially restricted diffusion of a pore confined fluid, a larger fraction of the fluid molecules will sense this restriction with increasing diffusion time. Hence, the effective diffusivity D will decrease with increasing diffusion time. For long diffusion times, D will approach a limiting value, corresponding to the long-range diffusivity limit. Using genera l physical arguments it can be shown that for short diffusion times the following equation applies[27].

$$\frac{D(t_D)}{D(0)} = 1 - \frac{4}{9\sqrt{\pi}}\frac{S}{V}\sqrt{D(0)t_D} - \frac{S}{6V}\frac{1}{R_0}D(0)t_D + \frac{\rho}{6}\frac{S}{V}t_D \qquad \text{(A2)}$$

where $1/R_0$ represents the curvature of the restricting geometry and ρ defines the surface relaxation strength. For even shorter diffusion times, the above equation simplifies further to;

$$\frac{D(t_D)}{D(0)} = 1 - \frac{4}{9\sqrt{\pi}}\frac{S}{V}\sqrt{D(0)t_D} \qquad \text{(A3)}$$

[27] P.P. Mitra, Sen, L.M. Schwartz, Phys. Rev. B, 1993, 47, 8565

Appendix B. A general approach to spectral analysis (two-spin system)

As pointed out in the previous section, the "n+1"-rule is valid as long as the chemical shift difference δ (Hz) between the nuclei is large compared to the coupling constant J between them, i.e., $\Delta\delta$ (in Hz) >> J. When $\Delta\delta$ (in Hz) ≈ J, the intensity distribution of the peaks will not be as predicted by the "n+1"-rule. The positions of the peaks are changed and the multiplet may contain additional peaks. Before considering some simple cases, we need to discuss the nomenclature.

Spins with the same chemical shift have the same letter in the alphabet. Spins that are separated by small chemical shift differences have letters that are close in the alphabet. Some examples: A_2, AB and AX. A_2 and AX will give first order spectra: A_2 - singlet, AX - two doublets. AB will give a more complex spectrum, which we will now calculate. We start with two spins, 1 and 2, which generate four spin-functions according to:

$$f_1 = |\alpha\alpha> \qquad f_2 = |\alpha\beta> \qquad f_3 = |\beta\alpha> \qquad f_4 = |\beta\beta> \tag{B1}$$

Actually, we should have written $\alpha(1)\beta(2)$ to identify the two nuclei 1 and 2, however, to simplify, the first wave function in each pair is assigned to spin 1 and the second one to spin 2). The Hamiltonian takes the form:

$$\hat{H} = \hat{H}_Z + \hat{H}_J \tag{B2}$$

By writing the operator in frequency units (Hz):

$$\hat{H}_Z = \nu_1 \bar{I}^z_1 + \nu_2 \bar{I}^z_2 \tag{B3}$$

ν_1 and ν_2 define the chemical shift (Hz) of the two spins. The term $\hat{H}_J$ in Eq B2 which defines the coupling Hamiltonian can be written:

$$\hat{H}_J = J\, \bar{I}^z_1\, \bar{I}^z_2 + (J/2)(\bar{I}^+_1\, \bar{I}^-_2 + \bar{I}^-_1\, \bar{I}^+_2) \tag{B4}$$

By introducing the raising and lowering operators (i = $\sqrt{-1}$):

$$\bar{I}^+ = \bar{I}^x + i\bar{I}^y \quad \bar{I}^- = \bar{I}^x - i\bar{I}^y \tag{B5a}$$

$$\bar{I}^+|\alpha> = 0,\ \bar{I}^+|\beta> = |\alpha>,\ \bar{I}^-|\alpha> = |\beta>,\ \bar{I}^-|\beta> = 0 \tag{B5b}$$

we will look for solutions of the Schrödinger equation ($\hat{H}\left|\Psi_i\right\rangle = E_i\left|\Psi_i\right\rangle$) of the form:

$$|\Psi_j> = \sum_{i=1}^{4} c_{ji}\left|f_i\right> \text{ for } j = 1,2,3,4 \tag{B6a}$$

From the theory of linear algebra, we can find the energies (E_i) by solving the following "secular" determinant:

$$\begin{pmatrix} H_{11}-E & H_{12} & H_{13} & H_{14} \\ H_{21} & H_{22}-E & H_{23} & H_{24} \\ H_{31} & H_{32} & H_{33}-E & H_{34} \\ H_{41} & H_{42} & H_{43} & H_{44}-E \end{pmatrix} = 0 \qquad \text{(B6b)}$$

with $H_{ij} = \langle f_i | H | f_j \rangle$

The solution to Eq 4.9b (see Exercises 4.1 – 4.4):

$$\begin{aligned} E_1 &= -V/2 + J/4 & |\Psi_1\rangle &= |\alpha\alpha\rangle \\ E_2 &= -C/2 - J/4 & |\Psi_2\rangle &= \cos\theta|\alpha\beta\rangle + \sin\theta|\beta\alpha\rangle \\ E_3 &= C/2 - J/4 & |\Psi_3\rangle &= -\sin\theta|\alpha\beta\rangle + \cos\theta|\beta\alpha\rangle \\ E_4 &= V/2 + J/4 & |\Psi_4\rangle &= |\beta\beta\rangle \end{aligned} \qquad \text{(B6c)}$$

We have introduced the parameters C, V and θ to simplify the equations:

$$V = \nu_1 + \nu_2 \qquad \text{(B6d)}$$

$$C = \sqrt{(\nu_1 - \nu_2)^2 + J^2} \qquad \text{(B6e)}$$

$$\sin 2\theta = J/C \ (\Leftrightarrow \cos 2\theta = (\nu_1 - \nu_2)/C) \qquad \text{(B6f)}$$

The calculated spectrum will consist of 4 lines, symmetrically distributed about the mean value $1/2(\nu_1 + \nu_2)$. The frequencies and intensities are given in the Table 1.

Table 1. *Frequency and relative intensity of the resonances within an AB-spin system*.

Transition (n m)	Frequency (E_n-E_m)	Relative intensity
2 1	$(V - C - J)/2$	$(1 - \sin 2\theta)/4$
4 3	$(V - C + J)/2$	$(1 + \sin 2\theta)/4$
3 1	$(V + C - J)/2$	$(1 + \sin 2\theta)/4$
4 2	$(V + C + J)/2$	$(1 - \sin 2\theta)/4$

We will discuss two limiting cases.

Case 1: $(\nu_1 - \nu_2) >> J$

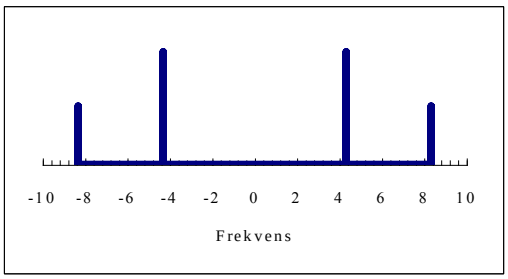

Figure 4.3

Then $C = (\nu_1 - \nu_2)/2$ and $\theta = 0$. The spectrum consists of two doublets. One doublet is centred at ν_1 with a distance between the two lines equal to J. The other doublet is centred at ν_2 with the same distance J between the two lines. All lines have the same intensity when $(\nu_1 - \nu_2) >> J$. The figure shows the calculated spectrum for J = 4 and $(\nu_1 - \nu_2) = 3J$. The intensity of the outer lines is reduced.

Case 2 $\nu_1 = \nu_2$

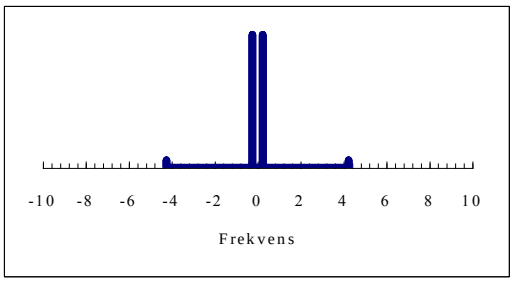

Figure 4.4

Then C = J and $\theta = \pi/4$The spectrum is then a singlet. The figure shows the calculated spectrum for J = 4 and (ν_1 - ν_2) = J/2. Compared to case 1 we see that the outer lines disappear when the chemical shift (ν_1 - ν_2) gets small compared to the coupling constant J. The distance between the two outer lines is J can be found directly from the spectrum and reads:

$$J = (\nu_1-\nu_2) = (\nu_3-\nu_4) \qquad \text{(B7a)}$$

The value of the chemical shift can be calculated from this equation:

$$\delta(\text{in Hz}) = \sqrt{(\nu_1 - \nu_4)(\nu_2 - \nu_3)} \qquad \text{(B7b)}$$

To check that the four lines really belong to an AB-quartet we can test the assumption by calculating the intensity distribution. In an AB quartet the intensity ratio of the inner lines and the outer lines is (ν_1-ν_4) / (ν_2-ν_3).

References

Claridge, Timothy D.W.: *High-Resolution NMR Techniques in Organic Chemistry*. Pergamon 1999. The book is used in KJM 4250 Organic NMR spectroscopy.

Freeman, Ray: *Magnetic Resonance in Chemistry and Medicine*. Oxford University Press 2003. This is book with almost no formulas.

Grant, David M. and Harris, Robin K Ed.: *Encyclopaedia of NMR Volume 1 Historical Perspectives*. Wiley 1996

Hornak, Joseph P.: *The Basics of NMR*. http://www.cis.rit.edu/htbooks/nmr/nmr-main.htm A book with animations with a lot of literature references.

Slichter, Charles P.: *Principles of Magnetic Resonan*ce. 3. Edition Springer (1990). A classical text (updated) with many formulas and literature references.

Vlaardingerbroek, Marinus T. and den Boer, Jacques A. *Magnetic Resonance Imaging. Theory and Practice*. Springer 1999.

R.F. Karlicek and I.J. Lowe, *J. Magn. Res*., **1980**, 37, 75)
R.M. Cotts, M.J.R. Hoch, T. Sun and J.T. Markert, *J. Magn. Res*., **1989**, 83, 252)